UPPSALA
UNIVERSITET

UPTEC X20001
Examensarbete 30 hp
Juni 2020

A study of protein aggregation processes using Dynamic Light Scattering

Validation of the technique and experimental trial with an active pharmaceutical ingredient

Cornelia Arnroth

UPPSALA
UNIVERSITET

Teknisk- naturvetenskaplig fakultet
UTH-enheten

Besöksadress:
Ångströmlaboratoriet
Lägerhyddsvägen 1
Hus 4, Plan 0

Postadress:
Box 536
751 21 Uppsala

Telefon:
018 – 471 30 03

Telefax:
018 – 471 30 00

Hemsida:
http://www.teknat.uu.se/student

Abstract

A study of protein aggregation processes using Dynamic Light Scattering

Cornelia Arnroth

Protein pharmaceuticals is one of the fastest growing class of therapeutics today. However, they pose a lot of challenges in production lines due to their poor stability. Protein aggregation is one of the most common results of protein instability and is a risk factor regarding the quality of therapeutics.

This master thesis at RISE focused on validating the techniques Dynamic Light Scattering (DLS) and multi angle DLS (MADLS) with respect to detection of aggregation. The model protein B-lactoglobulin was used to assess the robustness and accuracy of DLS. A comparison between two instruments from Malvern, Zetasizer Nano (2006) and Zetasizer Ultra (2018) was done with respect to DLS. It was determined that they were in many ways equivalent, but the newer model Ultra was favourable due to reduced noise and its ability to detect a lower concentration of aggregates. MADLS produced more precise results which is reflected in narrower distributions and has a higher sensitivity than DLS with regards to separating particles near in size. Both techniques proved sensitive enough to differentiate between aggregates and native protein.

Experimental trials were performed with an active pharmaceutical ingredient, API. The experimental trials with the API aimed to investigate what conditions and surface-interfaces that might pose a risk for aggregation. Despite efforts put in creating an environment where aggregation could be monitored, aggregation could not be established. Measurements with the API generated less reliable results due to noisy data and a lack of reproducibility between individual measurements.

Handledare: Linnea Enstedt och Ulla Elofsson
Ämnesgranskare: Maria Selmer
Examinator: Erik Holmqvist
ISSN: 1401-2138, UPTEC X20001
Tryckt av: Uppsala

Detektera proteinaggregering med dynamisk ljusspridning

- En populärvetenskaplig sammanfattning

Av Cornelia Arnroth

Den medicinska marknaden expanderar hela tiden med nya innovationer och läkemedel som släpps på marknaden. Ett aktuellt och växande område inom medicin är proteinläkemedel. Protein syntetiseras i alla levande celler och utför livsviktiga funktioner i organismer gällande generell hälsa och överlevnad. Proteinfloran ansvarar för att hålla oss vid liv genom att exempelvis läka sår och försvara kroppen mot infektioner. Ett annat sätt att se på det är att jämföra den mänskliga kroppen med ett vandrande medicinskåp. Det är därför inte förvånande att proteinläkemedel härstammar från levande organismer och utgörs av proteiner så som antikroppar, hormoner och enzym (Cox 2007).

Protein har använts som läkemedel sedan 1920 när insulin introducerades. Sen dess har massproduktion av proteinläkemedel stött på hinder vad gäller att hitta förhållanden där proteiner är stabila (Leurs *et al*. 2015). Proteinaggregering är det vanligaste resultatet av proteininstabilitet och definieras som polymerisering av proteiner och är inte önskat i den slutliga administrerade produkten. Aggregat sänker verkningsgraden av läkemedlet och kan aktivera immunförsvaret (Berrill *et al*. 2011). Tekniker för att detektera aggregering är därför avgörande för att säkerställa kvalitén av läkemedlet.

I sin naturliga miljö är protein veckade i tredimensionella former som är essentiella för deras egenskaper och funktioner. Proteinstrukturen är känslig och dynamisk vilket gör den väldigt lättpåverkad av miljöförändringar såsom temperatursvängningar, ändrat pH och/eller salthalt (Wang *et al*. 2010). Förändringar i proteinveckningen kan resultera i exponering av reaktiva grupper som kan leda till nya interaktioner vilket kan resultera i aggregering (Figur 1) (Blake *et al*. 2015). Detta fenomen utgör ett problem inom det medicinska området och mycket kraft läggs därför på att kartlägga vilka förhållanden som är gynnsamma för proteinstabilitet och vilka som utgör en risk.

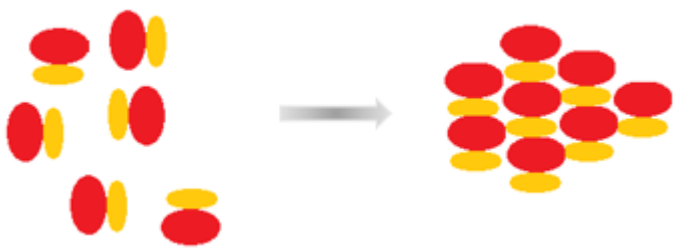

Figur 1 En schematisk illustration av proteinaggregering

Att etablera en robust och snabb metod för att utvärdera kvalitén på proteinläkemedel är därför viktigt. Dynamisk ljusspridning (eng. DLS) användes som valideringsteknik i det här projektet. Med DLS exponeras provet för en ljusstråle som sprids när den träffar en partikel, i det här fallet ett protein. Det spridda ljuset fångas upp av en detektor som transformerar signalen till en partikelstorleksfördelning (eng. PSD) som är en funktion av partikelns storlek (Stetefeld *et al*. 2016). I princip använder sig tekniken av att mäta hur länge en partikel är kvar på samma ställe, och då mindre partiklar rör sig snabbare än stora ser PSDs olika ut beroende på storlek. Principen kan därmed vara användbar för att detektera aggregat då de är större än protein i nativt stadie.

Projektet visar att DLS var en pålitlig metod när ett stabilt modellprotein användes, men att data var mindre pålitligt när mätningar gjordes på en farmaceutisk aktiv substans. Fortsatta experiment behöver göras för att fastställa i vilka sammanhang tekniken fungerar.

Table of contents

Abbreviations

AC	Adaptive Correlation
API	Active pharmaceutical ingredient
DLS	Dynamic light scattering
MADLS	Multi-angle dynamic light scattering
PDI	Polydispersity index
PSD	Particle size distribution

1. Introduction

The first protein to be administered as a drug on the market was insulin in the 1920s (Quiazon & Cheikh 2012). Today protein pharmaceuticals are the fastest growing class of therapeutics and have expanded to encompass four major groups: hormones, enzymes, antibodies and vaccines (Cox 2007). However, they pose a lot of challenges in analysis and characterization due to their diversity and intrinsic chemical and physical properties which makes them very sensitive to environmental changes (Solá and Griebenow 2009). The production line is also affected by the challenges in purification, storage and delivery since the structure of proteins are dynamic and generally unstable (Leurs *et al*. 2015). Protein aggregation is one of the most common results of protein instability and is a risk factor regarding the quality of the therapeutics (Berrill *et al*. 2011). Protein pharmaceuticals are active in specific configurations, i.e. when properly folded and in some cases correct/native oligomeric state. Aggregated states can in some cases work therapeutically but are generally recognized as deleterious to function, quality and performance (Roberts 2014). It is therefore of great interest to map what kind of conditions that enable or prevent, to any extent, aggregation of protein pharmaceuticals. Detection of aggregation is also an important pillar in the progress of understanding the aggregation process and could play a big role in solving the current problems with protein pharmaceuticals.

1.1 Protein aggregation and properties affecting it

Protein aggregation is defined as proteins interacting with each other causing polymerization to form soluble or insoluble aggregates (Roberts 2014). Proteins aggregate through different pathways such as chemical linkage or degradation, partially or fully unfolded proteins interacting and polymerizing or through self-association (Wang *et al*. 2010). Which phenomenon that drives aggregation can be very different and are often dependent on protein properties and/or the formulation (Berrill *et al*. 2011).

Interactions responsible for folding and stability of a protein are not static but are in constant balance and competition with each other, such interactions are for example intra- and intermolecular interactions (Price & Nairn 2009). Important intramolecular forces between amino acids are hydrogen bonding and van der Waal interactions. The dynamic nature of proteins makes them very susceptible to changes in the environment such as temperature shifts, altered pH or ionic strength and pressure (Wang *et al*. 2010). Thermal induction derives from altering the vibrational motion of the atoms and the diffusion coefficient of the protein. Decreasing or increasing the temperature can therefore destabilize the protein and promote aggregation (Elofsson 1996). Electrostatic properties of the sample is another factor that is crucial when studying aggregation. pH is directly responsible for net charge on the surface of the protein which affects the level of repulsion between proteins (Wang *et al*. 2010). Intramolecular interactions are also dependent on charge since repulsion amongst residues of the protein can lead to partial unfolding and exposure of hydrophobic groups (Wang & Roberts 2018).

Unfolded intermediates may be present under native conditions but increase in number if the environment favours or forces the protein to change conformation (Fink 1998). Conformational

changes may expose hydrophobic residues which are normally buried within the core of the protein or activate reactive residues such as cysteine groups which promote protein-protein interaction and will ultimately lead to aggregation (Blake *et al*. 2015).

1.2 Heat-induced aggregation of ß-lactoglobulin

ß-lactoglobulin, ß-lg, is a major protein component in milk serum (constituting > 50% of total whey protein) and occurs in two different variants, A and B (Kelly *et al*. 2009). They are both 162 amino acids long and differ only at two sites, 64 and 118 which is Asp and Val for ß-lg A and Gly and Ala for ß-lg B. It has five cysteine residues of which four form disulphide bonds (Cys^{106}-Cys^{119} and Cys^{66}-Cys^{160}) and one remains as a free thiol group (Cys^{121}) (Bauer & Hansen 1998). The free thiol group is buried in the hydrophobic core of the protein in its native state and is thus prevented from being reactive (Sava *et al*. 2005). Thermal treatment promotes unfolding of the protein, exposing the free thiol group and making it reactive. It can then stimulate the formation of new disulphide bonds between or within ß-lg, which is an important process in the heat-induced aggregation process (Croguennec *et al*. 2004).

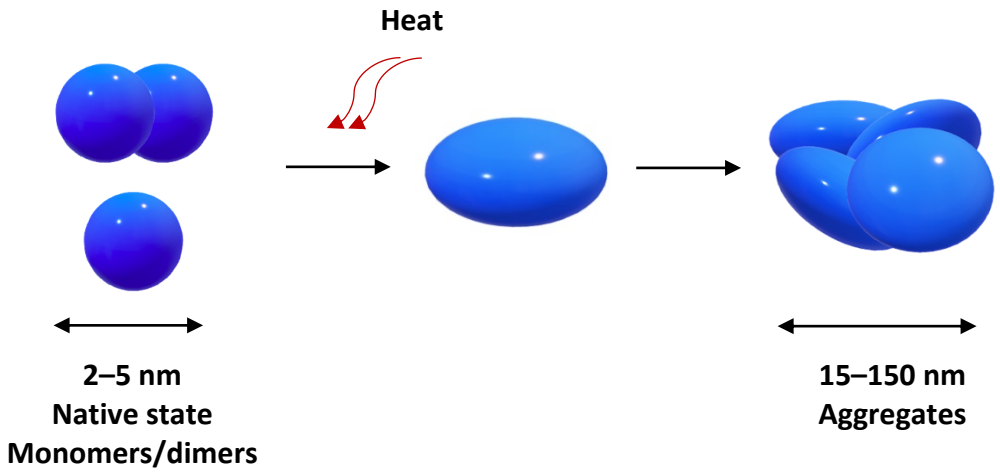

Figure 2 A schematic illustration of thermal induction of aggregation with the model protein ß-lg. *In its native state the protein has an average diameter of 2-5 nm. Adding heat to the sample leads to partial unfolding of the protein, unfolded ß-lg polymerize and produces aggregates.*

β-lg is suitable as a model protein for studying aggregation since the aggregation process is controllable due to thermal induction.

1.3 Dynamic Light Scattering

Dynamic light scattering (DLS) is a technique that enables size measurements of macromolecules. The instruments used for measuring DLS in this project are Zetasizer Nano (2006) and Zetasizer Ultra (2018) from Malvern, the latter being a newer model with the option of subjecting a sample to multi-angle DLS (see section 1.4). The technique is based on exposing the sample to a monochromatic wave of light that scatters upon encountering the molecules. The scattered light is captured by a detector and transformed to a particle size distribution curve (PSD) which is a function of the particles' size (Stetefeld *et al*. 2016).

DLS is based on Brownian motion, i.e. particles' movement and collisions with solvent molecules causing energy transfer that have a greater effect on smaller molecules. Due to this, smaller components move faster than those greater in size which means that the size of a particle can be derived from its speed in the solution. The Stokes-Einstein equation (Equation 1) combines light scattering and diffusion behaviour of a particle to derive its size

$$D = \frac{k_B \times T}{3\pi \times \eta \times L} \times F_D \qquad (1)$$

where D is the diffusion coefficient, η is the solvent viscosity, k_B the Boltzman constant, L is the length and T is the temperature. F_D depends on the shape of the particle and is denoted as the geometrical constant. The diffusion coefficient is based on a hypothetical spherical shape of the particles being measured (for spheres $F_D = 1$) even though particles in a solution are rarely spherical and static in their structure (Arenas-Guerrero *et al*. 2018).

Moreover, scattered light waves superpose and produce a resultant wave where the amplitude is the sum of the individual waves. The light waves can cancel out (destructive phases) or amplify each other (constructive phases), an event called interference, and generate a detectable signal which is recorded and monitored by a detector (Figure 3) (Ockenga 2011). Due to the movements of the molecules and interference of the scattered light the intensity of the scattered light is not constant but fluctuating. The pattern of intensity is used in a correlation function which basically describes how long a particle is situated at the same spot within the solution. As the particle moves away, the function exponentially decreases until it has reached the baseline, indicating that the molecule is no longer in close proximity to where it originally was. Since smaller molecules move faster than larger ones, their correlation functions will look different, i.e. giving a slower decay for a larger particle.

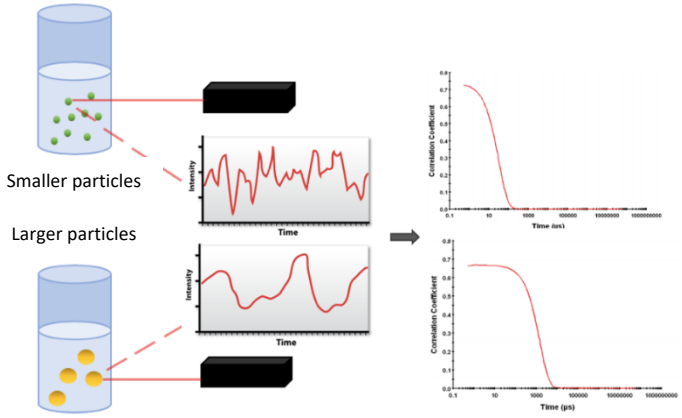

Figure 3 DLS is based on Brownian motion where the size of the particles correlates to the speed with which they move. *Smaller particles move with greater speed than larger ones and will thus generate different correlation functions. The correlation functions are transformed to PSDs.*

PSD shows the distribution of particles in a sample arranged according to size or mass and the frequency in which they occur. The width of the distribution is denoted as polydispersity index (PDI). A sample is considered monodisperse if the PDI is less than 0.2. Different weights can be given to a particle depending on the chosen distribution, i.e. signals are amplified with different scaling. Number-weighted distribution utilizes a counting principle where each particle is given the same weight, disregarding their size. Volume-weighted distributions is based on volume of the particles and is thus weighted $(size)^3$. In the Intensity-weighted distribution the contribution of each particle is proportional to $(size)^6$ (Malvern Panalytical 2020). From the size analysis two different parameters with respect to size are produced: z-avg and peak mean. Z-avg is the calculated size of the whole sample and is considered the most reliable size parameter when a sample is monodisperse. Peak mean generates the mean size for each peak of a measurement and is thus more reliable when a sample is polydisperse. Relevant parameters for this report are listed in Table 1.

Table 1 Relevant parameters generated by DLS listed along with a short description of their meaning

Parameter	**Meaning**
Polydispersity index, PDI	Estimate of the divergence of PSDs
Z-avg	Average size (nm) of the whole sample
Peak mean	Mean size (nm) of each peak
Particle size distribution, PSD	Size distributions derived from the techniques

The newer instrument, Zetasizer Ultra, uses an updated correlation function called Adaptive Correlation (AC). AC reduces signal to noise by applying algorithms that can distinguish measurement data not representative of particles in the sample (Malvern Panalytical 2018).

1.4 Improvements with Multi-angle DLS

Multi-angle DLS (MADLS) increases the resolution compared to single-angle measurements by combining scattering patterns from several angles (13º, 90º, 173º). The generated distributions of each angle are combined and produce a PSD from multiple angles. When a sample is not monodisperse, the resolution obtained with DLS might not be good enough for a sufficient distinction between the different states of molecules, whereas the increased sensitivity of MADLS can separate particles near in size. With a poor resolution, important information could be lost or hard to interpret (Malvern Panalytical 2018).

2. Methods

The Master Thesis can be divided into two sections: Validation and Experimental trials. The validation was conducted with the aim to asses two different Malvern instruments, Zetasizer Nano and Zetasizer Ultra, in their ability to produce reproducible and robust results. In the validation process the model protein β-lg was used. For the experimental trial an active pharmaceutical ingredient (API) was used.

2.1 DLS measurements

Instruments used for standard DLS was Zetasizer Nano and Zetasizer Ultra. MADLS could only be measured with Zetasizer Ultra. All size measurements were done in triplicates to produce more robust results. Average curves were made from the three curves directly in the Zetasizer Nano instrument, but the Zetasizer Ultra does not have that editing tool so average curves were done in Excel. Settings on the Nano instrument were set to default except Equilibrium time: 30 s, Number of runs: 3, Number of repeats: 11. Settings on the Ultra were set to default except Equilibrium time: 30 s. These settings will be denoted as standard and can be assumed to have been used unless anything else is stated.

2.2 Validation with β-lg

Different treatments of β-lg were used to produce a variety of aggregated states. Samples were then measured by DLS with both instruments to compare the generated size distributions. Zetasizer Ultra was also used to measure samples with MADLS, and the results were compared to DLS. Moreover, Transmission electron microscopy (TEM) imaging was kindly performed on samples in NextBioForm's collaboration with Vironova. The TEM images were used to validate the DLS-measurements.

2.2.1 Preparation and induction of aggregation of β-lg

All stocks of β-lg were made to a concentration of 10 ± 1 mg/mL from which dilution series were made (1 mg/mL, 0.1 mg/mL and 10 µg/mL). β-lg was dissolved in a 50 mM phosphate buffer with 0.02% Sodium Azide (NaAz, a preservative), for a detailed description of preparations and calculations see Appendix 1. Buffer and samples were filtered through a 0.22 µm filter to remove any particles that were not properly dissolved, before inducing aggregation.

As standard treatment to achieve aggregation, 2 mL of stock solution was heated to a temperature of 70 ± 1˚C for 1 h in a water bath. Samples were then quenched on ice for 10 min and after equilibration to room temperature (~15 min) measured with DLS and MADLS. Previous studies show that the size of the aggregates depends on temperature and heating time (Elofsson 1996). To assess the ability of DLS to differentiate between aggregate populations, β-lg was heated for 1 h in 75˚C and 80˚C as well as 2 h in 70 ˚C. A flow scheme of mentioned experiments with β-lg is illustrated in Figure 4.

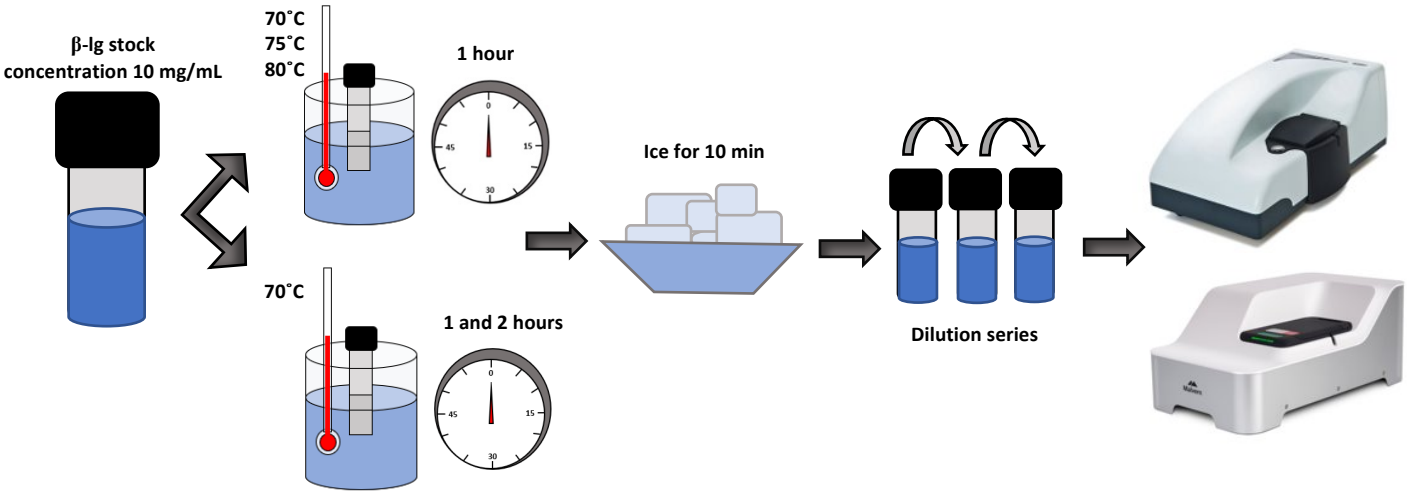

Figure 4 A flow scheme of different experiments done with ß-lg

For every measurement of aggregated β-lg, unheated β-lg was measured as to compare aggregated and non-aggregated samples but also to assess the quality of the sample before inducing aggregation.

2.2.2 Sensitivity of the instruments

To assess the instruments' capacity to separate between different populations in a sample, heat-treated and unheated β-lg were mixed to a final concentration of 1 mg/mL. Different percentages of heated sample (5, 10, 20 and 30) were tested as to find the lowest level of aggregates that produced clear signals and where aggregation could be detected. Measurements were performed with both DLS and MADLS to asses sensitivity of the techniques, e.g. ability to separate the populations. Results will then be compared to TEM images as to analyse resolution differences between the techniques (Note! Images for this experiment have not yet been taken and will therefore not be presented in the report).

2.2.3 Monitoring heat induced aggregation with Zetasizer Ultra

The Zetasizer Ultra instrument can be used to heat a sample directly in the instrument which made it possible to monitor the aggregation process and trend curves were then created in Excel. Forty-seven size measurements resulted in 1 h of heating time in the instrument. Temperature was set to 70˚C and equilibration time to 0, the rest of the settings according to standard settings (see section 2.1). After establishing that aggregation did occur when heating β-lg in the instrument, samples were heated in parallel in a water bath of 70˚C. Samples from the water bath were removed from heating as size runs on the instrument started showing population shifts, schematic illustration in Figure 5. These samples were then quenched on ice bath for 10 min and after equilibration to room temperature measured with DLS and MADLS (Zetasizer Ultra) and compared to corresponding size measurement from sample heated in instrument. Samples were sent to Vironova for TEM imaging; however, images have not yet been taken and will thus not be a part of this report.

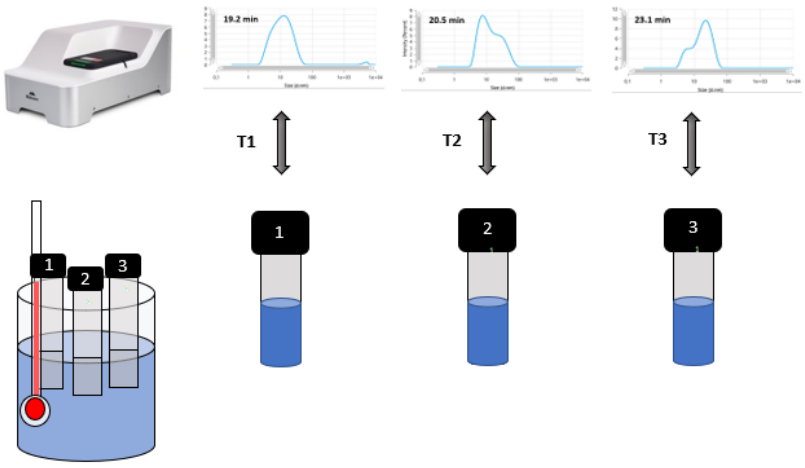

***Figure 5 Samples with B-lg were heated in water bath in parallel to heating in Zetasizer Ultra instrument**. As PSDs started to indicate population shifts in the instrument samples were taken out of the water bath. Samples from water bath were then measured in instrument and PSDs were compared.*

2.2.4 Lowest detection limit

Proteins are expensive so it was of interest to identify the lowest volume and concentration of sample that could be used for a reliable result. Malvern provides a capillary cuvette that takes up to 3 µL, compared with disposable cuvettes taking 1 mL (Figure 6). Detection limits were compared between the two measurement volumes. The capillary cuvette is not compatible with the Zetasizer Nano instrument, so measurements were done with the Zetasizer Ultra. With the capillary cuvette, MADLS cannot be performed so all measurements were done with DLS.

***Figure 6 Two different cuvettes were used to investigate lowest limit of detection.** To left: Disposable 1 mL cuvette (Wikimedia commons 2017). To right: Capillary cuvette (Malvern Panalytical 2018).*

For each volume, concentrations of 1 mg/mL, 0.5 mg/mL, 0.1 mg/mL and 50 µg/mL were tested, and the quality of the measurements assessed. To determine the reliability of the

measurements the correlograms, PSDs, size parameters (z-avg and peak mean) and PDIs were analysed.

2.3 Experimental trial with an API

The API was exposed to surface interfaces to assess risk factors regarding aggregation. Three different pH were tested to asses pH dependence for aggregate formation.

2.3.1 Silanization of silica beads

To obtain hydrophobic surfaces boro-silica beads (diameter 1 mm) were silanized. Beads were washed in Piranha solution (>90% H_2SO_4 and 30% H_20_2 with a 3:1 ratio) for 30 min with a stirrer to clean and OH-activate the surfaces. The beads were rinsed extensively with water and then dried in an oven (110ºC) until completely dry. Beads were then incubated with stirring in silane solution (Trichloro[octyl]silane added to toluene (99%) to final concentration of 1%) for 30 min. For cleaning of the beads, they were washed three-fold with 99% EtOH and rinsed with Milli-Q. The beads were kept in 99% EtOH until usage. The silanization protocol used in this project was based on papers by McGovern *et al* (1994) and Weetal (1996).

2.3.2 Treatments of the API

Working concentration of the API was 3 mg/mL. The API was dissolved in 10 mM phosphate buffer with 0.02% NaAz filtered through 0.22 µm filter. The API was stored in freezer at - 20˚C in freeze-dried aliquots and was taken out 10 minutes before preparation, for detailed preparation and calculations see Appendix 2. The sample was measured unfiltered and filtered (filtration with centrifugation filter with cut-off at 50 kDa) and DLS measurements between the treatments were compared.

For experiments with the API three different pH were tested: 6.5, 7 and 7.4. For each pH four vials were prepared according to Table 2. All vials were pre-rinsed with Milli-Q.

Table 2 Different treatments of the API were performed to assess surface induced aggregation

Treatment/surface	**Preparation**
Filled vial, i.e. no air	Vial filled with sample all the way to the top, surface tension observed above bottleneck.
Hydrophobic beads, no air	~5 g silanized boro-silica beads (surface area ~716 cm^2) were added to vial. Sample (~1.5 ml) was then added all the way to the top (surface tension above bottleneck).
Air and air bubbles	2 mL sample was added to vial, which left ~3mL air in the vial. When vial was shaken, air bubbles/foam formed.
Untreated API	No treatment after API had been dissolved. Sample did not fill the whole vial, i.e. air was present but no physical treatment (shaken/tilting table) was performed on the sample.

The vials were shaken by hand (except for the vial with native sample) for 10 s and were left for 1 h before measurements. The vials were then placed on a tilting table (15 turnovers per min), see Figure 7, for 1 hour before being measured with DLS and MADLS again.

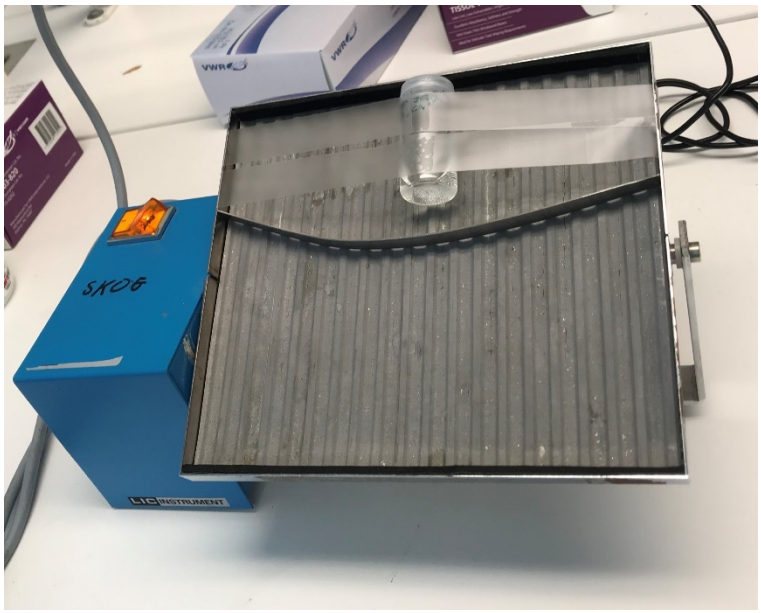

Figure 7 Set up for API samples placed on tilting-table. *Turnover speed was 15/min.*

3. Results

Several experiments with the model protein β-lg were conducted to determine the performance of the techniques and will be described under validation experiments. Experiments conducted with an API will be described under experimental trials.

The validation with β-lg was divided into several sub-experiments to assess the capacities of the techniques. Standard DLS was compared between the instruments (Zetasizer Nano and Ultra) and to MADLS regarding precision and repeatability (section 3.1.1). The ability of the techniques to distinguish aggregates generated by different treatments was investigated by testing different heating times and temperatures (section 3.1.2). By mixing heated and unheated β-lg to different ratios, the capacity of DLS and MADLS to separate the two populations was tested (section 3.1.3). It was also possible to monitor the aggregation process with the Zetasizer Ultra instrument. The robustness of the method was assessed and compared to standard heating of β-lg, e.g. water bath of 70˚C (section 3.1.4). Finally, lowest limit of concentration for detection was tested with two different cuvettes (section 3.1.5).

For the experimental trial with an API, one section covers the pH dependence of aggregation formation (section 3.2.1) and one section the impact of surface interfaces (section 3.2.2) for inducing aggregation.

3.1 Validation with β-lg

3.1.1 Comparison between DLS and MADLS

Initial experiments were done with the aim to assess any possible differences between the results produced by DLS of the two instruments' as well as a comparison with MADLS. Samples with standard treatment (70˚C for 1 h) and unheated samples were first examined in the Zetasizer Nano instrument to establish a distinction between the two, e.g. aggregated versus non-aggregated, Figure 8A & B.

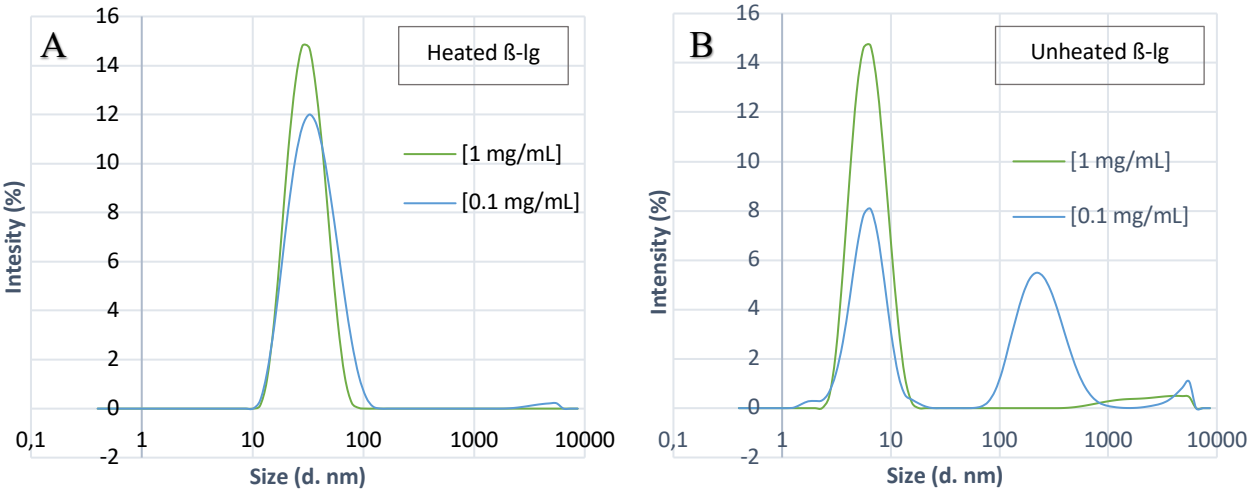

Figure 8 Initial measurements with the model protein B-lg, measured in ZS-Nano*. Two concentrations, 1 and 0.1 mg/mL. A: Heated B-lg, detection of aggregation for both concentrations. B: Unheated B-lg. Concentration 1 mg/mL produce a peak at a size representative of native β-lg (5 nm). PSD from measurement with [0.1 mg/mL] displays one peak for native protein and one at a greater size, which is not representative to the protein.*

PSDs in Figure 8 look different between the samples, which is expected. The z-avg values derived from the measurements differ between the samples: ~29 nm for heated and ~6 nm for unheated, which shows that the technique can separate particles of the size range used in this project. The PSD generated from the unheated protein shows three peaks for 0.1 mg/mL but only one peak for 1 mg/mL, Figure 8B. The concentration 0.1 mg/mL is therefore denoted as unreliable since peaks at greater size are not representable of the protein in the sample.

Repeatability of measurements was assessed by comparing individual curves (i.e. not average curves) of heated β-lg with standard treatment and standard deviations of z-avg and peak mean are listed in Table 3. PSDs are displayed in Figure 9.

Table 3 Repeatability between measurements. *Standard deviations of size measurements (nm) between individual curves made from triplicates*

Instrument (Zetasizer)	Sample [1 mg/mL]	Z-avg (nm)	σ(Z-avg)	Peak mean by Intensity (nm)	σ(Peak mean)
Ultra	Heated	28.8	0.26	32.4	0.33
Nano	Heated	28.53	0.086	32.32	0.66
Ultra	Unheated	5.91	0.071	6.52	0.11
Nano	Unheated	6.12	0.36	6.57	0.086

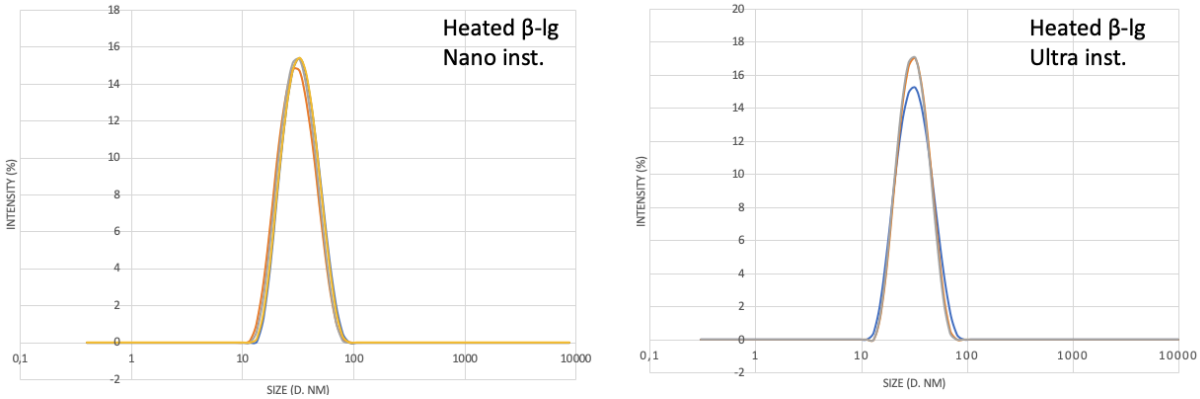

Figure 9 Reproducibility between measurements. *Individual curves for one measurement (triplicates), one in Zetasizer Ultra and one in Nano. Individual curves align with each other.*

The robustness and repeatability of measurements of β-lg is high. Individual measurements of a sample with β-lg (heated and unheated) produce PSDs and correlograms that follow each other with almost perfect fit. Unheated β-lg needs to have a concentration of 1 mg/mL or above to produce good data.

Heated and unheated β-lg-samples were examined in the Zetasizer Ultra instrument with DLS and MADLS. The measurements are plotted with Size by Intensity distributions obtained with the Zetasizer Nano, Figure 10 & 11. PSDs of unheated β-lg display peaks of greater size which are denoted as noise.

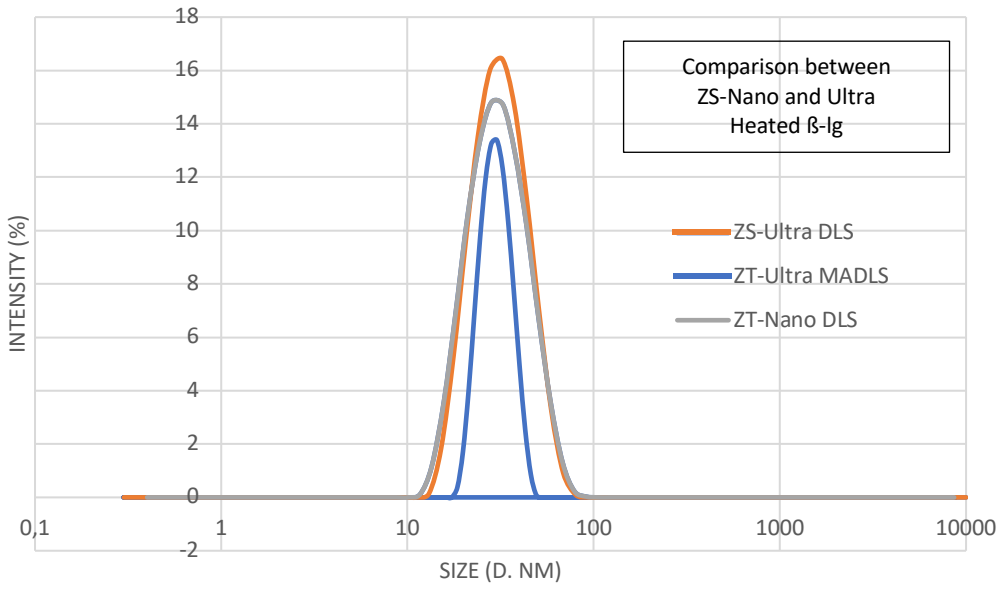

Figure 10 Compared measurements of B-lg in two different instruments: Zetasizer Nano (DLS) & Zetasizer Ultra (DLS & MADLS). *The peaks cover the same size range but MADLS produce a more narrow distribution (blue) and thus a more precise estimate of particle sizes.*

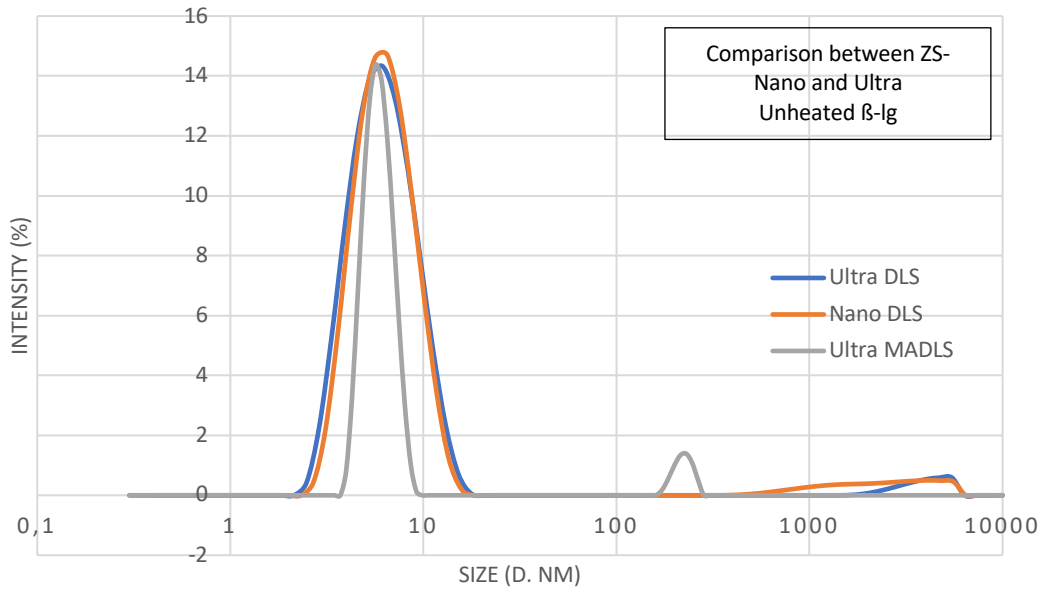

Figure 11 Compared measurements of unheated B-lg by Zetasizer Ultra (DLS & MADLS) and Nano (DLS). *The peaks cover the same size range but MADLS produce a more narrow distribution (grey) and thus a more sensitive estimate of particle sizes. Peaks at greater sizes are not representative of sample particles but denoted as noise.*

The width of the peaks varies between DLS and MADLS, the latter generating the narrowest peak. A narrower distribution indicates a more precise estimation of particle sizes. The PDIs are listed in Table 4 along with derived sizes. MADLS does not produce a PDI which is a disadvantage of the technique since the index is used as quality assurance of a measurement.

Table 4 Particle size values obtained from measurements with Zetasizer Ultra (MADLS and DLS) and Nano instrument (DLS). *Z-avg and PDI is not produced when utilizing MADLS and is thus not listed. All sizes agree but MADLS gives a smaller size estimate for both heated and unheated ß-lg.*

INSTRUMENT	Z-AVG MEAN (NM)	PEAK MEAN BY INTENSITY (NM)	PDI
		Heated β-lg	
ZS-NANO DLS AVG	30.01	32.3	0.108
ZS-ULTRA DLS AVG	29.1	32.8	0.106
ZS-ULTRA MADLS	Not shown	30.0	Not shown
		Unheated β-lg	
ZS-NANO DLS AVG	6.55	6.66	0.25
ZS-ULTRA DLS AVG	5.81	6.27	0.203
ZS-ULTRA MADLS	Not shown	5.33	Not shown

Samples were sent for TEM imaging at Vironova as to compare to the results from DLS and MADLS (Figure 12).

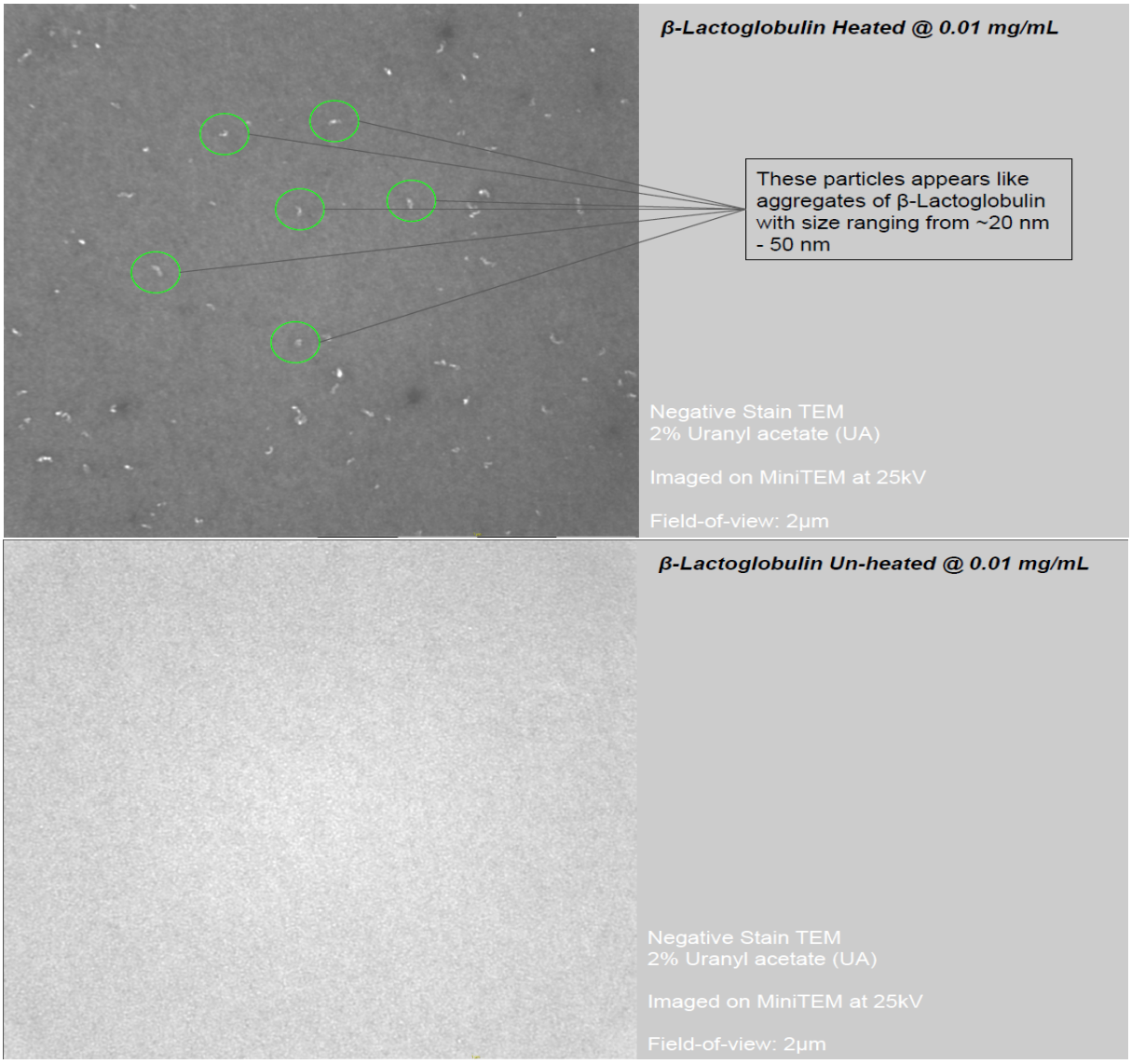

Figure 12 TEM images of heated (upper) and unheated (lower) ß-lg*. TEM images showed that unheated sample did not contain aggregates. Heated ß-lg displayed aggregates with a size range of 20-50 nm.*

From TEM images, the size of aggregates is estimated to ~20-50 nm compared to 13-79 for DLS (Ultra and Nano) and 17-52 for MADLS. Thus, the results generated by the orthogonal techniques agree with each other, supporting the reliability of the PSDs produced by DLS/MADLS, the latter being the most precise.

3.1.2 Varying the treatment of β-lg to study difference in aggregates

The size and shapes of aggregates can vary depending on which conditions they are induced. To assess the instruments ability to distinguish between aggregates produced by different treatments, two different heating times (1 and 2 h) and three different temperatures (70, 75 and 80˚C) were compared.

3.1.2.1 Comparing aggregate sizes at different heating times

Measurements were carried out with the Zetasizer Nano and Ultra instruments, and generated PSDs were plotted together, Figure 13 and 14.

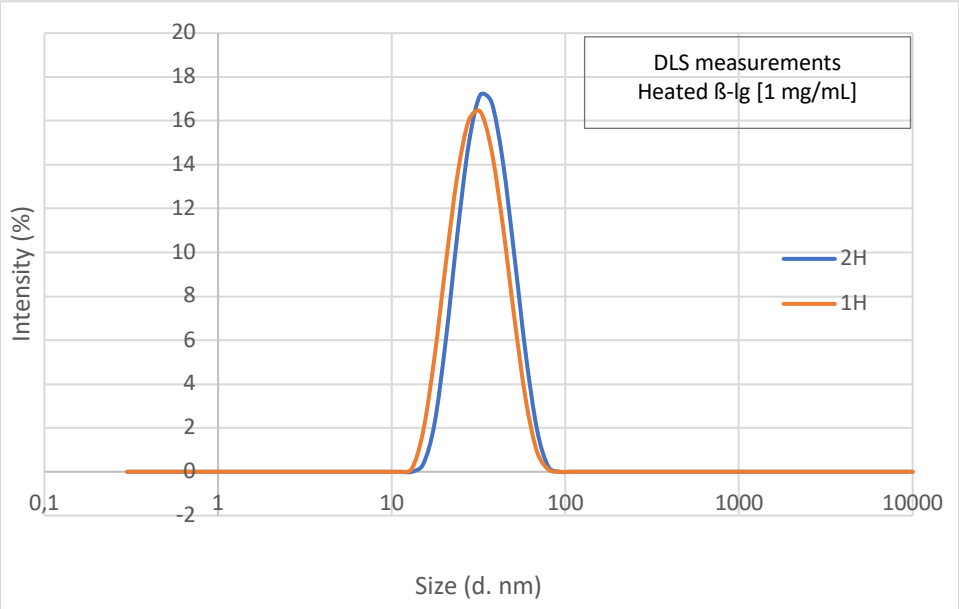

Figure 13 Comparison between heating times (1 vs 2 h) of B-lg. *No difference is observed between the treatments when measuring samples with DLS.*

When measuring with DLS there is no significant difference in generated PSDs, the calculated z-avg mean and peak mean by intensity all lie within 31 ± 2 nm and 35 ± 2 nm, respectively. With MADLS, however, the peak mean intensity does differ between the heating times, 30.1 and for 1 h and 34.3 nm for 2 h (Note that MADLS does not generate a z-avg). The results indicate that MADLS can make a better distinction between the two samples which is also reflected in the narrower peaks produced by MADLS (Figure 14).

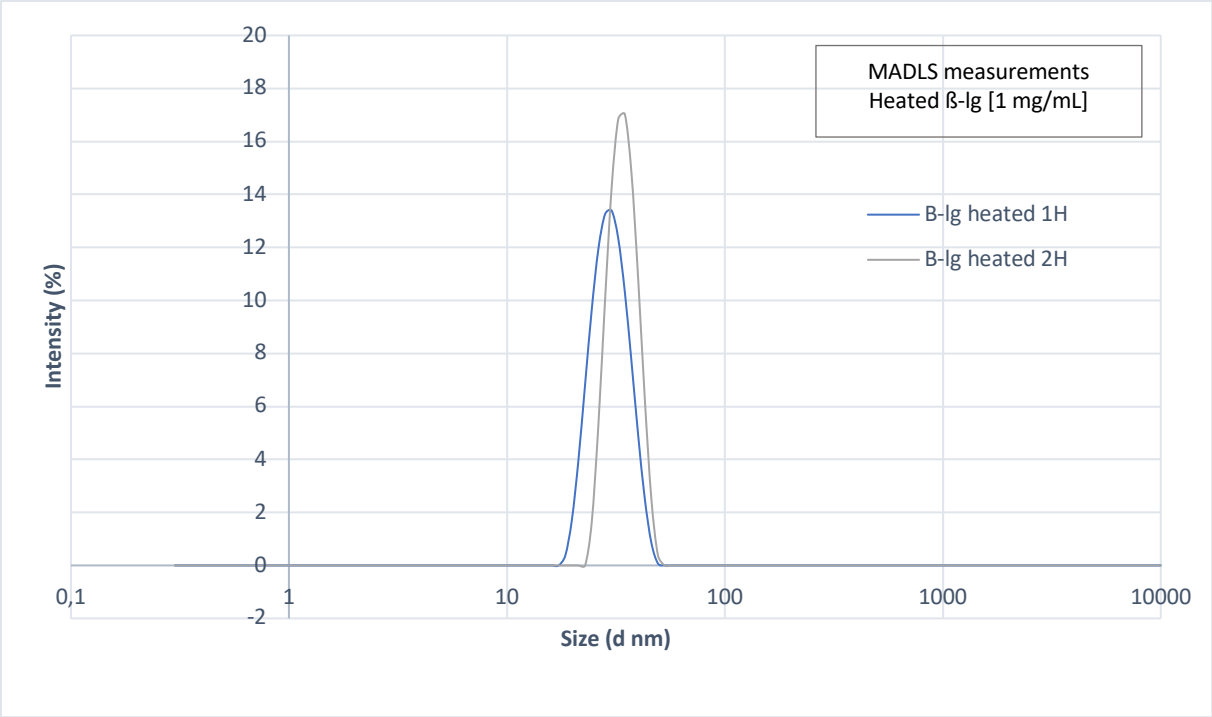

Figure 14 Comparison between two different heating times (1 and 2 h) of B-lg analyzed with MADLS. *The two PSDs are clearly different where heating time 2 h is slight shifted toward a bigger size distribution.*

3.1.2.2 Comparing aggregate size at different heating temperatures

To assess the ability of DLS and MADLS to detect differences in the size of aggregates, samples were heated at different temperatures, e.g. 70, 75 and 80˚C for 1 h and then analysed with the Zetasizer Ultra instrument. The generated Size by Intensity distributions are shown in Figure 15, for simplicity only MADLS measurements are displayed. There is a positive correlation between increased temperature and the size of aggregates, see Table 5, which can be detected with both MADLS and DLS.

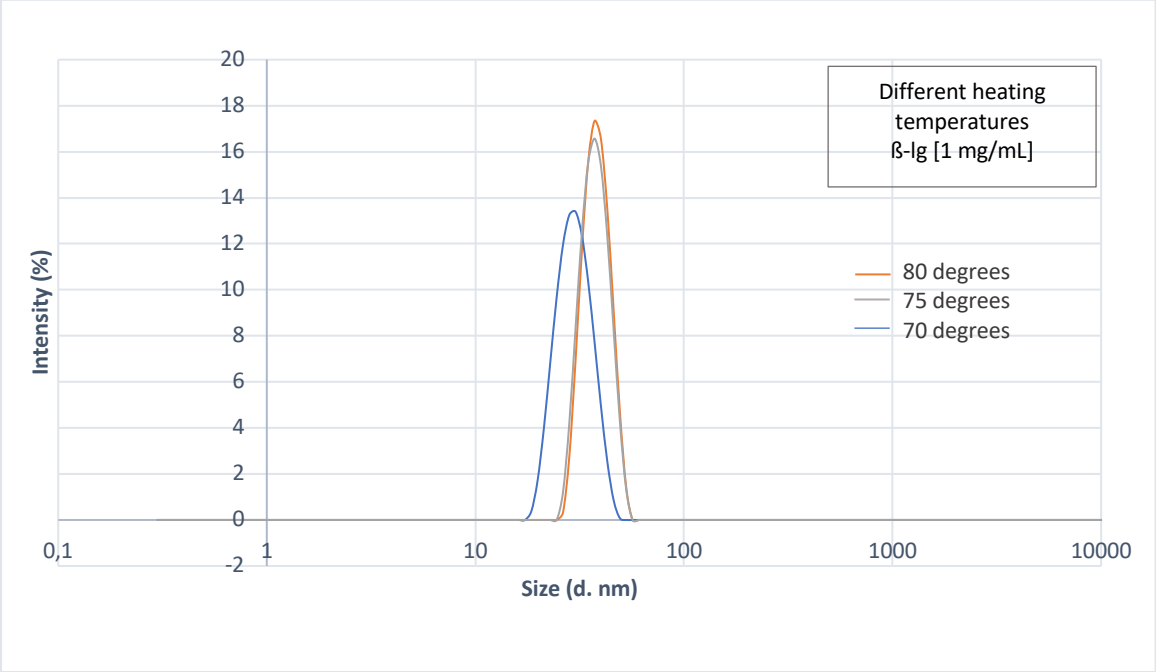

Figure 15 Three different temperatures (70, 75 and 80˚C) of B-lg were analyzed with MADLS. *The PSD of sample heated in 70˚C is visibly different from the other distributions. Increasing the temperature results in larger aggregates, and MADLS is sensitive enough to detect these differences.*

Table 5 Size of aggregates obtained at different temperatures*. Measured with DLS and MADLS*

TECHNIQUE	TEMPERATURE (˚C)	PEAK MEAN SIZE (NM)
DLS	70	32.8
MADLS		30.1
DLS	75	40.5
MADLS		37.2
DLS	80	44.1
MADLS		41.2

3.1.3 The ability of DLS and MADLS to identify populations in sample

To assure that the sample was polydisperse, heated β-lg was mixed with native protein, i.e. non-heated. By measuring a mixed sample, the resolution with respect to separation of the two populations of the instruments can be assessed and compared (Figure 16).

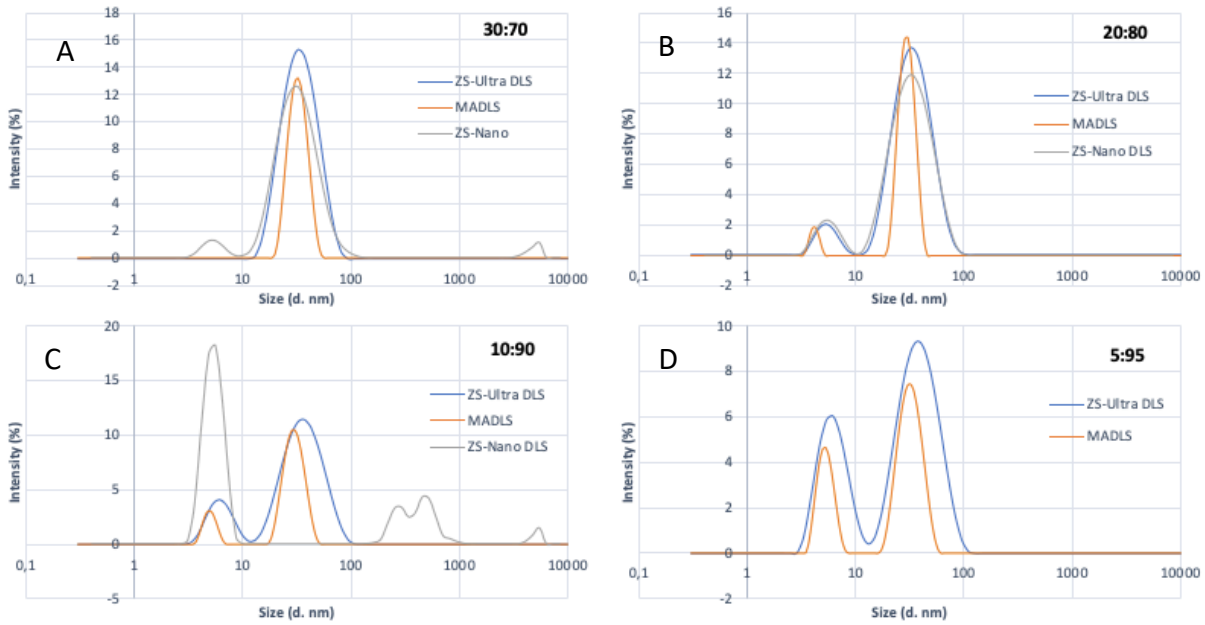

Figure 16 Heated and unheated B-lg were mixed as to ensure polydispersity. *Different concentrations of aggregates were tested.* ***A.*** *Zetasizer Nano is the only instrument that identifies native ß-lg.* ***B.*** *Both instruments identify the two populations, irrespective of DLS and MADLS.* ***C.*** *Zetasizer Nano did not generate a signal for aggregated ß-lg but peaks at greater size that are not representative of the protein. Due to the noisy PSD the Zetasizer Nano was not appropriate for measurements with a lower percentage of aggregates.* ***D.*** *The Zetasizer Ultra instrument produced clear results at 5% aggregates (both DLS and MADLS).*

Samples were measured with both Zetasizer Nano and Ultra, Figure 16. For measurements with ratio 30:70 the Zetasizer Ultra (DLS & MADLS) was incapable of detecting native ß-lg whereas the Zetasizer Nano produced a PSD with both native and aggregates protein represented. Zetasizer Nano produced a noisy PSD when reaching 10% heated and 90% unheated β-lg, but the Ultra instrument could go lower without the same noise (Figure 16C & D). The size difference between heated and unheated β-lg (5 nm vs 30 nm) is big enough for the resolution of DLS to separate the size populations, but MADLS can make better distinctions than DLS when size populations are closer in size, see Figure 18.

3.1.4 Monitoring heat-induced aggregation

Samples were heated directly in the Zetasizer Ultra instrument. The aggregation process could thereby be monitored and the increase in size of the aggregates was plotted against time (Figure 17). This method could be helpful when learning about a new protein's behaviour regarding aggregation if there is a suspicion that protein pharmaceutical is prone to aggregate at a certain temperature and/or in a specific formulation. Two measurements were made with ß-lg to control the reproducibility of the method and it was found that it is a robust approach due to the curves almost perfect fit to each other.

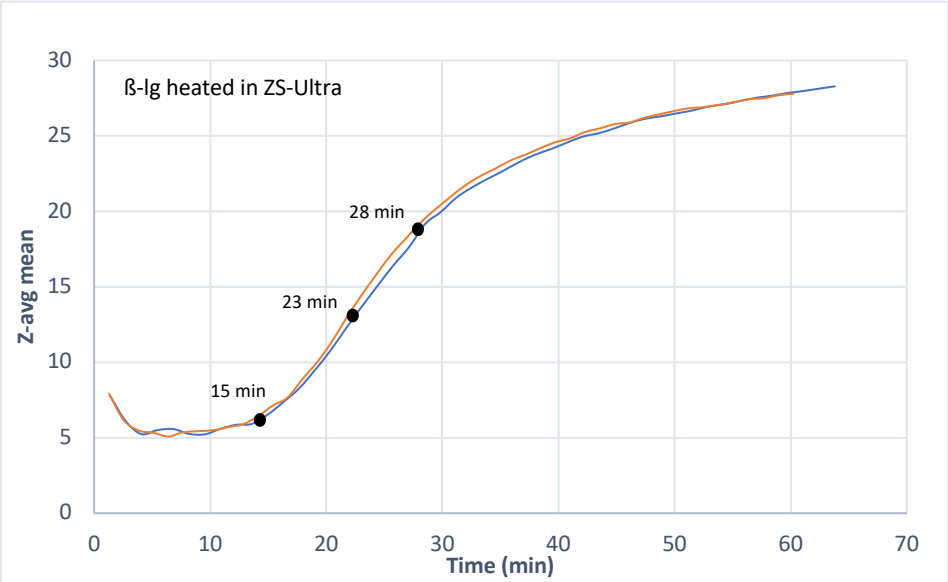

Figure 17 Heat induced aggregation of ß-lg could be monitored in Zetasizer Ultra. *The Z-avg mean values for each size measurement is plotted against time. The trend curve shows a clear correlation between aggregation and heating. According to the trend curve the lagging phase last for 12 min before aggregation starts. Time points (15, 23 & 28 min) marked on linear part of the trend curve represents heating times compared with ß-lg heated in water bath.*

Individual size measurements from the linear segment of the trend curve (Figure 17) show population shifts in the sample, e.g. progression from native state to aggregated. To assess if heating of the sample in the instrument is directly relatable to heating in a water bath, the two heating methods were done in parallel. When a population shift was noted from the size measurements a sample heated in water bath was removed and placed on ice. In total, three samples were heated in a water bath to compare with different steps in the population shift, heating times marked in Figure 17.

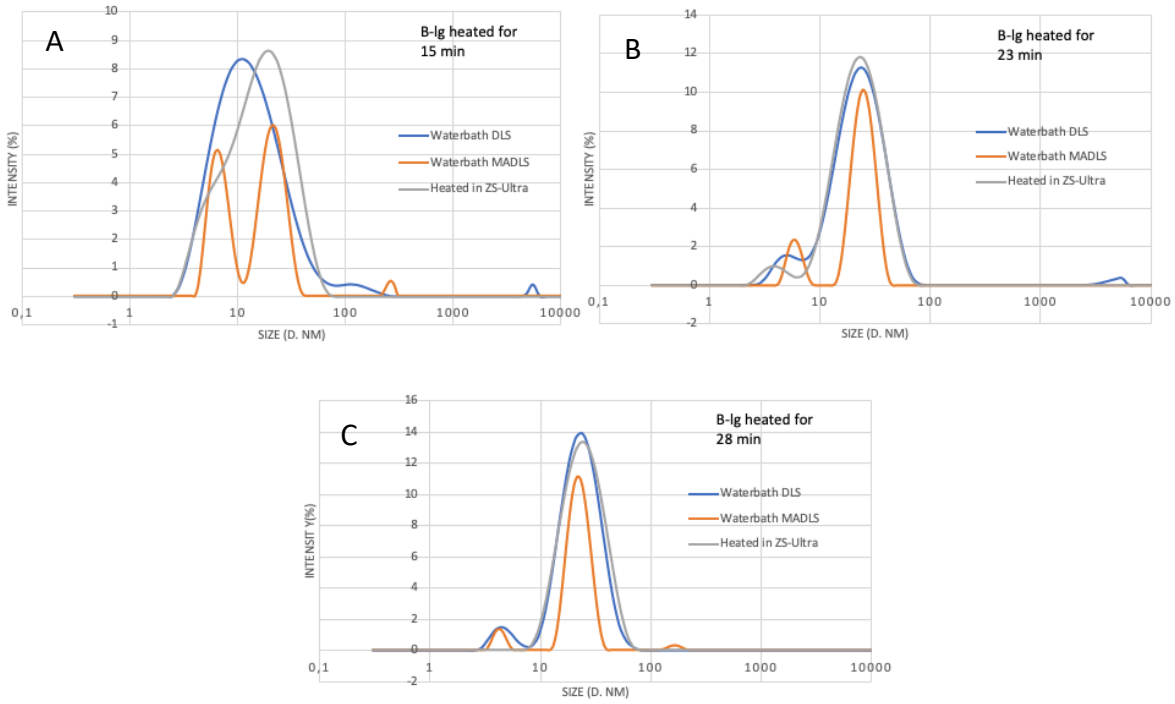

Figure 18 Samples were heated in 70˚C water bath in parallel with heating in Zetasizer Ultra instrument. *As population shifts was observed in the size runs of the instrument, samples were removed from water bath. PSDs from samples corresponding to the same time are plotted together and shows that 15 (**A**) and 23 (**B**) min resulted in the same general PSDs. MADLS can separate two populations in sample heated for 15 min. At 28 (**C**) min the sample heated in Zetasizer Ultra has fully shifted to aggregates whereas the sample from the water bath is still progressing.*

Based on the size distributions the methods agree at 15 and 23 min but deviate at 28 min. Sample heated in the instrument seems to have fully shifted to aggregates at 28 min whereas sample from water bath still shows a signal for unaggregated β-lg. Progression of the aggregation processes could be dependent on heating methods and sample volume. Sample volume heated in the Ultra instrument was 1 mL and in water bath 2 mL. The material of the vials in which heating took place were also different between the treatments, i.e. glass for water bath and acrylic cuvette in the instrument, which could affect aggregation. Samples heated in water bath were quenched on ice before measurements, which is likely to have an impact on aggregates.

3.1.5 Lowest limit of detection

Proteins are generally expensive, so using as little as possible for quality assurance and control is always of interest. Experiments for lowest limit of detection were therefore preformed with β-lg in its native and aggregated state. Decreasing concentrations were tested in two different cuvettes, disposable (1 mL) and capillary cuvette (3 µL) (Figure 19-21). The minimal volume was also of interest as to minimize the amount of protein used in DLS measurements.

Concentrations used were 1 mg/mL, 0.5 mg/mL, 0.1 mg/mL and 50 µg/mL. A sample with concentration 10 µg/mL was prepared but was excluded from the measurements as 50 µg/mL displayed poor quality.

All measurements generated approximately the same z-avg and peak intensity mean (Table 6), which indicates that the method is robust for a very low concentration but when comparing the correlograms it becomes apparent that quality decreases with concentration (Figure 19).

Table 6 Size values from measurements with two different volumes in decreasing sample concentration. *All sizes coincide except for one outlier (*). PDI is higher for unheated ß-lg.*

Heated β-lg				
Concentration	**Cuvette/ volume**	**Z-avg (nm)**	**Peak Intensity mean (nm)**	**PDI**
1 mg/mL	Capillary/ 3 µL	29.6	33.8	0.118
1 mg/mL	Disposable/ 1mL	29.8	33.6	0.106
0.5 mg/mL	Capillary/ 3 µL	29.6	33.4	0.132
0.5 mg/mL	Disposable/ 1mL	30	33.9	0.113
0.1 mg/mL	Capillary/ 3 µL	29.7	35	0.156
0.1 mg/mL	Disposable/ 1mL	30.1	33.2	0.133
50 µg/mL	Capillary/ 3 µL	28.4	33.5	0.196
50 µg/mL	Disposable/ 1mL	30.7	35.8	0.141
Unheated β-lg				
1 mg/mL	Capillary/ 3 µL	5.51	6.51	0.224
1 mg/mL	Disposable/ 1mL	95.9*	5.35	0.134
0.5 mg/mL	Capillary/ 3 µL	4.58	4.83	0.433
0.5 mg/mL	Disposable/ 1mL	5.73	6.41	0.215

*Probable pollutant in sample, should be considered as unrepresentative of particles in sample

The correlograms of measurements (Figure 19B) with the capillary cell get noisy when decreasing the concentration, so even though the values from Table 6 coincide with each other one should not go below the concentration 0.5 mg/mL since the samples with concentration 0.1 mg/mL and 50 µg/mL are not trustworthy on their own. A correlogram of good quality should display strong correlation at the beginning of the measurements (e.g. a flat curve), followed by an exponential decrease as the correlation decreases until the baseline is reached (Appendix 3). For measurements of heated β-lg with 1 mL aliquots, however, the correlogram keeps a good quality despite the decrease in concentration, Figure 19A. The lowest recommended concentration for measurements of heated β-lg with disposable and capillary cuvette is 50 µg/mL and 0.5 mg/mL, respectively.

Larger volumes need to be prepared when measuring 1 mL aliquots which means that lowering the concentration might still not lead to using less protein in total compared to samples run in capillary cuvette. Amount of protein used for measurements with recommended concentrations per volume are 50 µg (1 mL) and 1.15 µg (3 µL). Preparing a sample for measurement with the capillary cuvette however needs to have a concentration of 5 mg/mL which is higher than when utilizing a disposable 1 mL cuvette (50 µg).

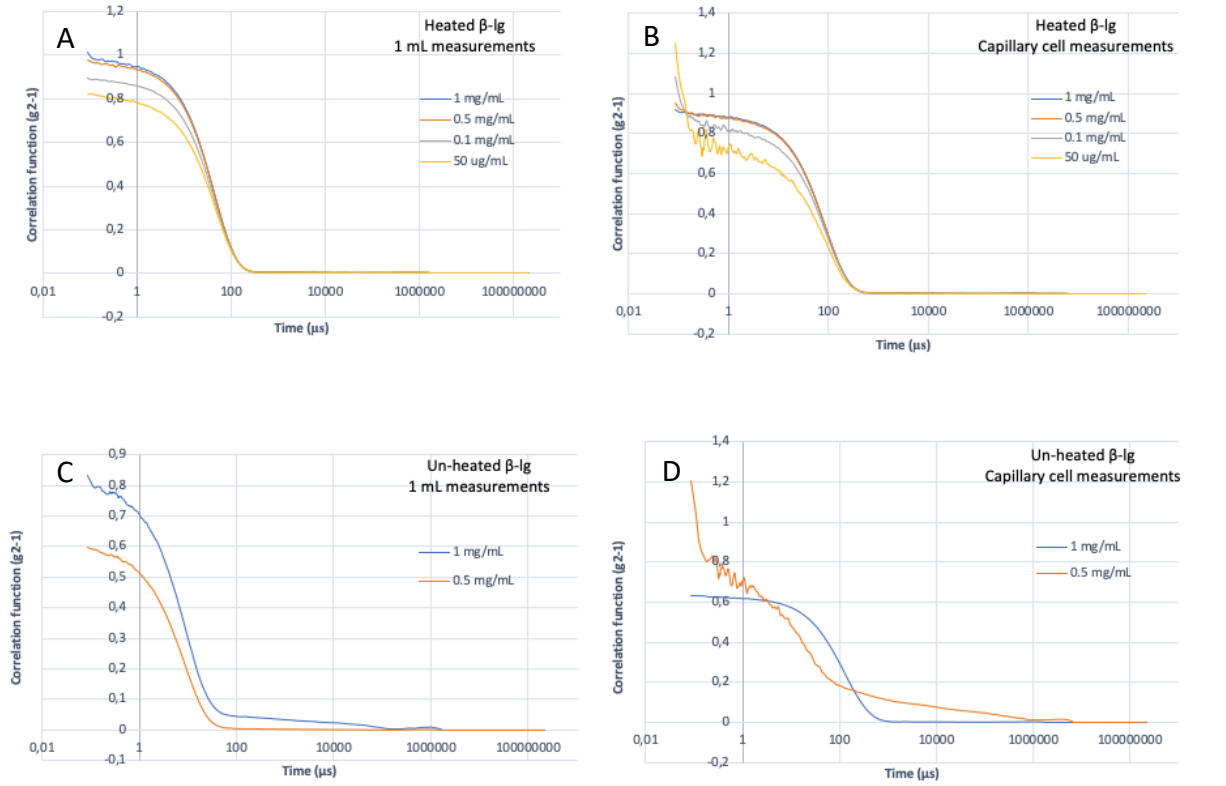

Figure 19 Correlograms of measurements with decreasing concentrations. A. *1 mL measurements of heated ß-lg show correlograms of good quality for all concentrations.* ***B.*** *Measurements of heated ß-lg with capillary cuvette is more sensitive to concentration. The quality of the correlogram drops at 0.1 mg/mL.* ***C****. Unheated ß-lg should not go below 0.5 mg/mL when using 1 mL measurements based on the correlograms.* ***D.*** *For measurements of unheated ß-lg with capillary cell one should not go below 1 mg/mL.*

It has already been established that for native β-lg, unreliable results are produced at a concentration of 0.1 mg/mL (Figure 8). Therefore, two concentrations were tested for unheated β-lg: 1 mg/mL and 0.5 mg/mL. As the correlograms indicate, a higher concentration (1 mg/mL) produces more reliable results when using the capillary cuvette (Figure 20B). For measurements with 1 mL, however, 0.5 mg/mL can be considered as reliable due to good quality of correlogram (Figure 19C) and a PSD with low noise.

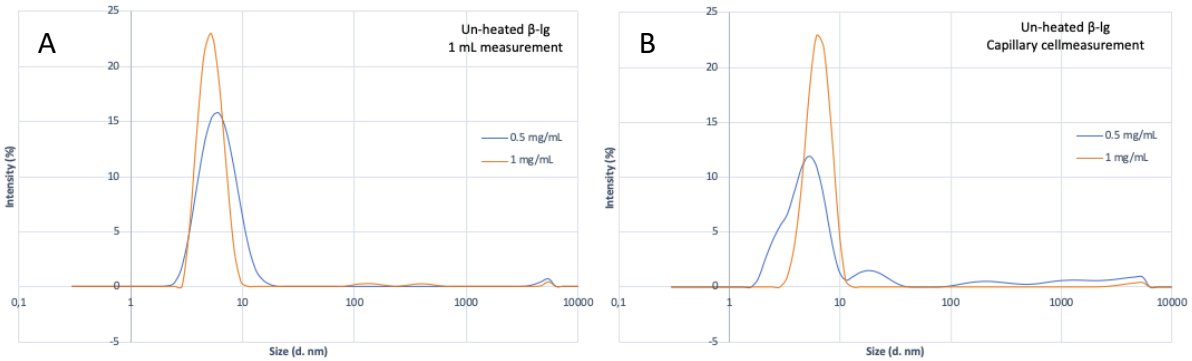

Figure 20 Size by Intensity distributions of unheated ß-lg*. 1 mL measurements* ***(A)*** *produce reliable results for both concentrations, but with the capillary cuvette* ***(B)*** *[0.5 mg/mL] the PSD is noisy and unreliable (e.g. peaks at greater size with considerable intensity signal).*

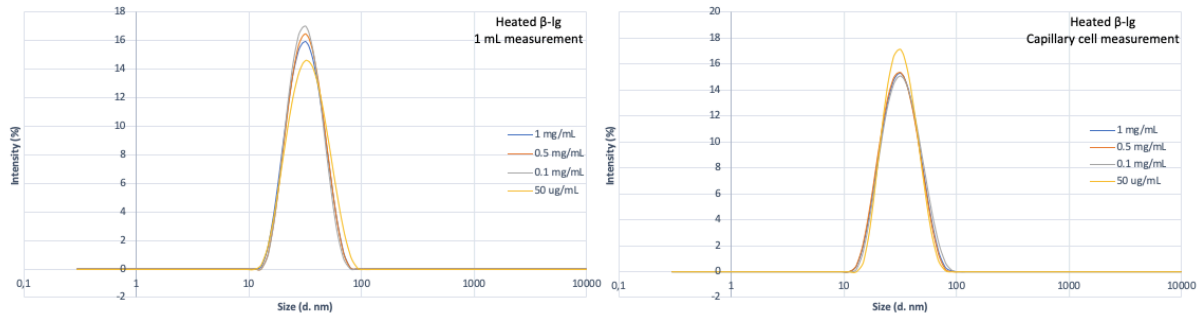

Figure 21 The Size by Intensity distributions for heated ß-lg. *PSDs for all concentrations and both cuvettes look trustworthy. The correlogram of the capillary cuvette, however, indicates that despite the PSDs one cannot trust [0.1 mg/mL] and [50 µg/mL].*

Size by Intensity distributions (Figure 20 & 21) and Table 6 shows that the sizes from each concentration do align around the same mean size (except one outlier, Table 6). For measurements with capillary cuvette, however, heated samples with the concentrations 0.1 mg/mL and 50 µg/mL and the unheated sample with concentration 0.5 mg/mL should not be counted as reliable on their own due to their poor correlograms (e.g. poor correlation at the start of the measurements).

3.2 Experimental trials with API

The measurements of the API with DLS were not as straight forward as when using the model protein β-lg. For the API (native and treated), the PSDs displayed several peaks without the ability to draw a conclusion around aggregation. The API was filtered through centrifugation filter to try and reduce the noise. Filtered and unfiltered samples were measured with a UV-spectrometer and DLS. Filtration did not improve the quality of the PSD curve (Figure 22) and a loss of about 30% of the API was derived from measurements of absorbance at 280 nm. Experiments with the API were therefore carried out without filtering the sample.

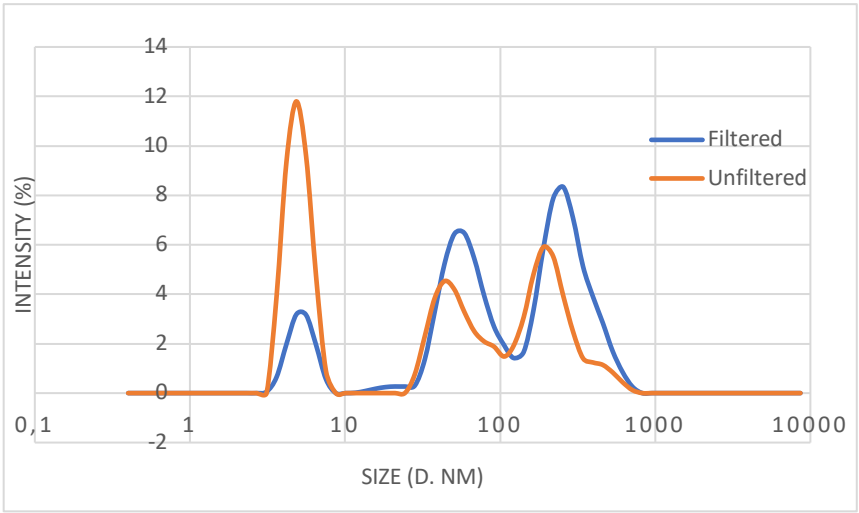

Figure 22 Filtered API did not produce a less noisy PSD. *No quality difference was observed by filtering the API through a centrifugation filter with 50 kDa cut off and there was a loss of 30% protein.*

3.2.1 pH dependence for aggregation formation of the API

API samples were prepared in three different pH: 6.5, 7.0 and 7.4. Intensity weighted distributions of untreated (i.e. neither shaken nor placed on tilting table) protein are displayed in Figure 23 along with one volume distribution. The first peak represents the native state of the protein (5 ± 0.5 nm), other peaks cannot be determined because each individual measurement looks very different.

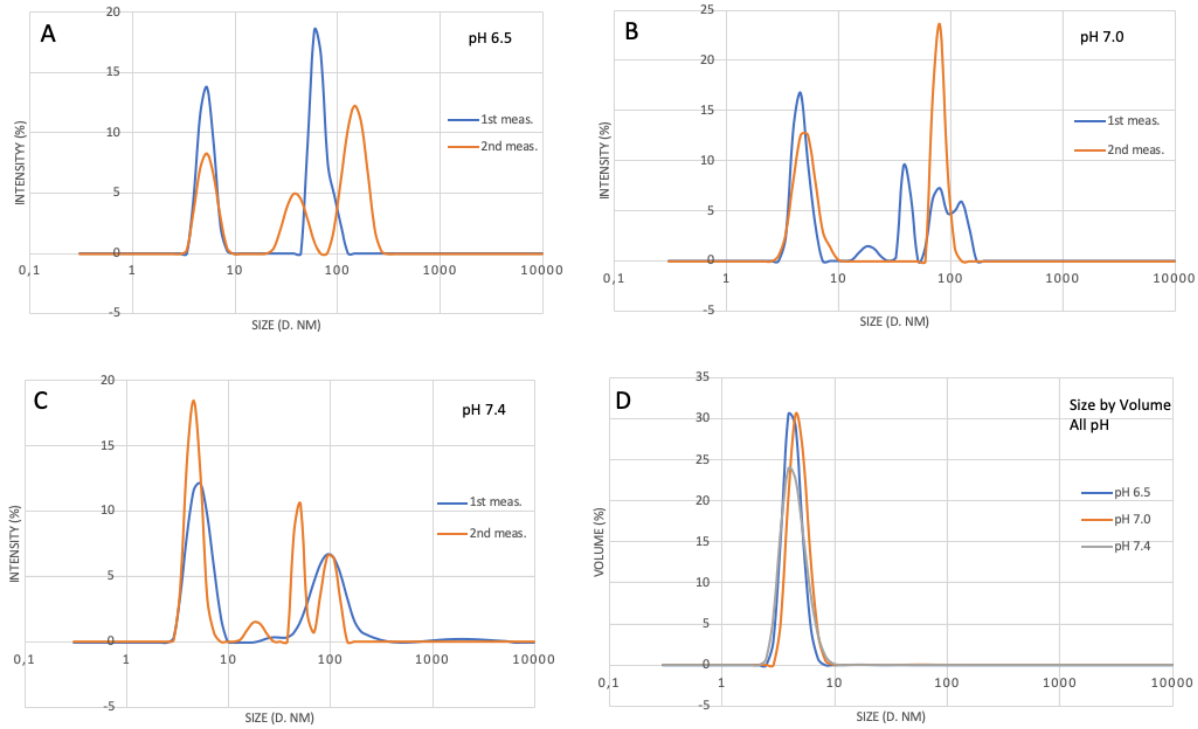

Figure 23 PSDs of untreated API in different pH. A. *API dissolved in pH 6.5.* ***B.*** *API dissolved in pH 7.0.* ***C.*** *APl dissolved in pH 7.4.* ***D.*** *Untreated/native samples of all pH plotted in Size by Volume distribution. Figure D indicates that all peaks in A-C above 10 nm should be regarded as false signals.*

The PSDs of native protein, i.e. untreated, generates several peaks. Figure 23A-D illustrates average curves made from triplicates. Triplicates did not align with each other but appeared to be drifting at peaks of greater size. Comparing the intensity (Figure 23A-C) and volume distributions (Figure 23D) indicates that if aggregates are present in the samples the amount is negligible, e.g. the peaks of greater size in the intensity weighted PSDs could be representative of aggregates but does not exceed the threshold for detection in the volume distribution.

When measuring untreated API one hour apart, the intensity at 5 nm was lower than the second measurement for sample with pH 6.5 (Table 7). As the size by volume distributions does not indicate clear aggregation, adsorption to vial surface could be an explanation to the decrease in intensity percentage (Table 7). Regarding the stability of the protein in different pH one could

argue that a decrease in intensity percentage in the peak representing native state (first peak ~5 nm) correlates to stability. The decrease in percentage means that protein transition to aggregates or adsorb onto surfaces.

Table 7 Percentages in intensity representing the native shape of the API compared between time points. *pH 6.5 show a clear decrease in intensity of native API. Changes in percentage of native API at pH 7.0 and 7.4 are negligible.*

PH	HOURS	NATIVE (%)	PDI	PEAK MEAN (NM)
6.5	1	41.6	0.454	5.24
	2	29.2	0.351	4.7
7.0	1	50	0.602	4.52
	2	51	0.64	5.05
7.4	1	54	0.365	5.86
	2	54.1	0.528	4.81

3.2.2 Impact of surface interface on aggregation

For each pH three treatments of the protein API were done: contact with hydrophobic beads, air bubbles and completely filled vial (i.e. no air, only vial can have effect). The samples were first shaken by hand for 10 s (sample denoted as shaken) and then placed on tilting table for 1 h (sample denoted as tilting table).

The hypothesis was that the API would adsorb to surfaces when shaken, leading to structural changes that could possibly progress as aggregation in the solution. When placed on a tilting table the adsorbed proteins would be in contact with proteins still in the solution, and thereby reveal the possibility of progression of aggregation. No aggregation could be detected with DLS and MADLS, but for the samples in contact with air at pH 6.5 and 7.0 displayed a decrease in native protein (Table 8). If not caused by aggregation, adsorption is a possibility and should be further investigated.

Table 8 Comparison of intensity representing native API*. The three treatments are listed (air-water interface, contact with hydrophobic beads and completely filled vial). For each treatment, the average value is listed.*

PH	TREATMENT	FILLED VIAL (%NATIVE)	AIR (%NATIVE)	HYDROPHOBIC BEADS (%NATIVE)
6.5	Shaken 10s	17.3	22.7	19.3
	Shaken + tilting table	27.4	11.2	21.7
7.0	Shaken 10s	39.8	33.3	24.5
	Shaken + tilting table	33.7	17.4	20.6
7.4	Shaken 10s	37	29.7	31.3
	Shaken + tilting table	40.3	26.8	32.5

The intensity percentages are calculated in the Zetasizer software. It should be noted that software for the Ultra instrument cannot make average curves, so the intensity percentages are taken from superimposing the curves (three curves per sample) on each other and use those values as an average.

The Size by Intensity and Size by Volume distributions combined indicates that peaks of greater size range in the intensity spectra are not true signals from the API but impurities from buffer or possible dust particles, Figure 24. The same result is observed for all treatments at all tested pH when comparing intensity and volume distributions (Appendix 5). For comparison, a Size by Volume distribution with β-lg where two populations can be seen is displayed in Figure 27.

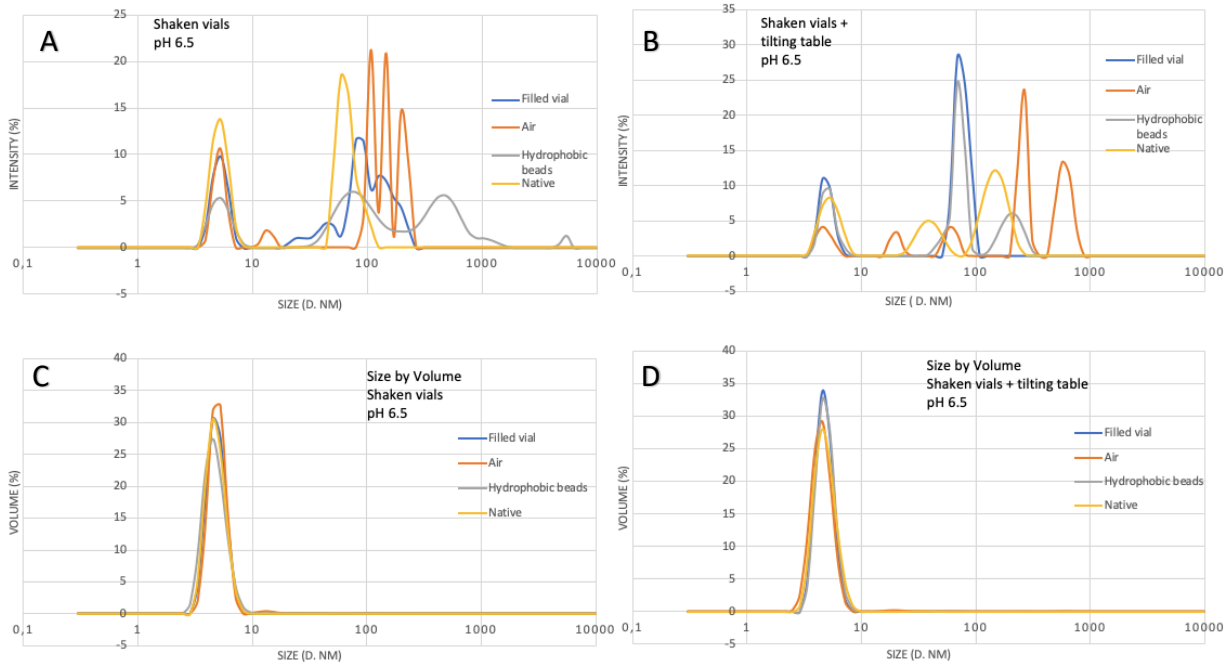

Figure 24 API in contact with different surfaces and in pH 6.5. A. *Size by Intensity distribution for samples that had been shaken for 10 s by hand.* ***B.*** *Size by intensity distribution for samples that had been on a tilting table for 1 h after being shaken.* ***C & D****. Size by Volume distributions display only one peak, aggregation cannot be established.*

From Table 8, the biggest decrease in percentage of protein in its native state occurred at pH 6.5. The results from Figure 24C and 24D supports the hypothesis of adsorption rather than aggregation with respect to loss of native protein.

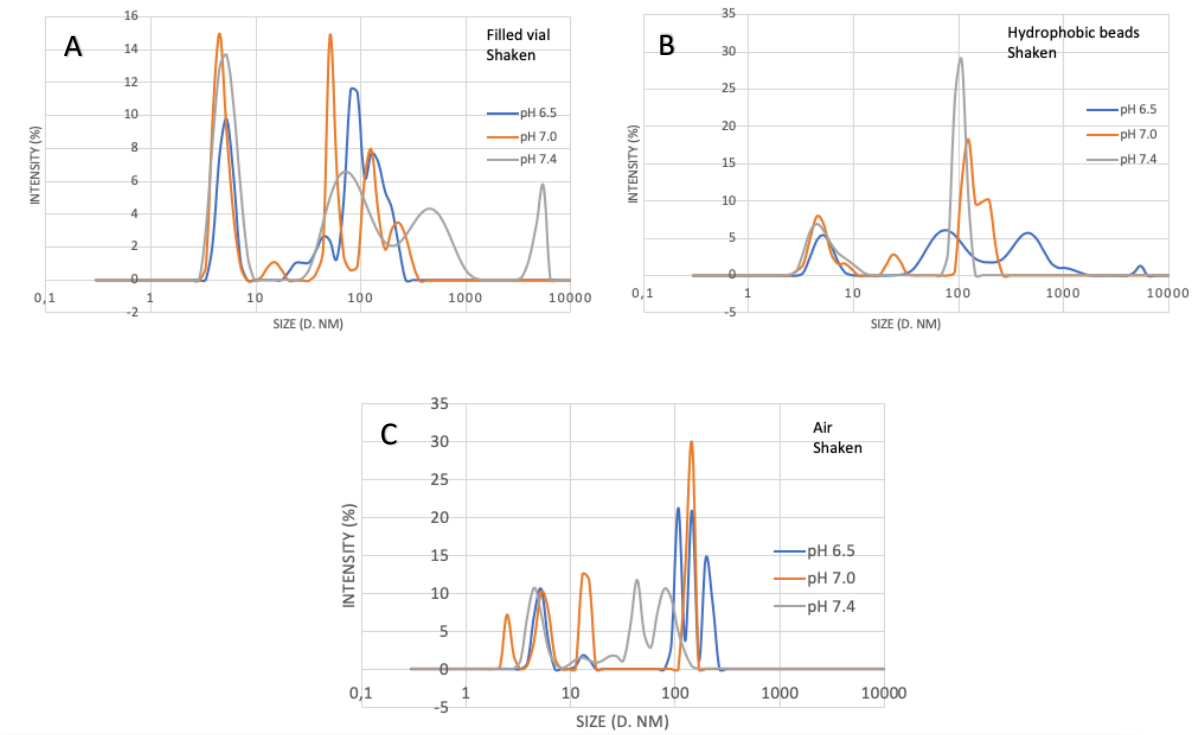

Figure 25 API with different surface interfaces and pH, all samples are shaken. A. *Completely filled vial (i.e. no air).* ***B.*** *Hydrophobic beads.* ***C.*** *Air-water interface*

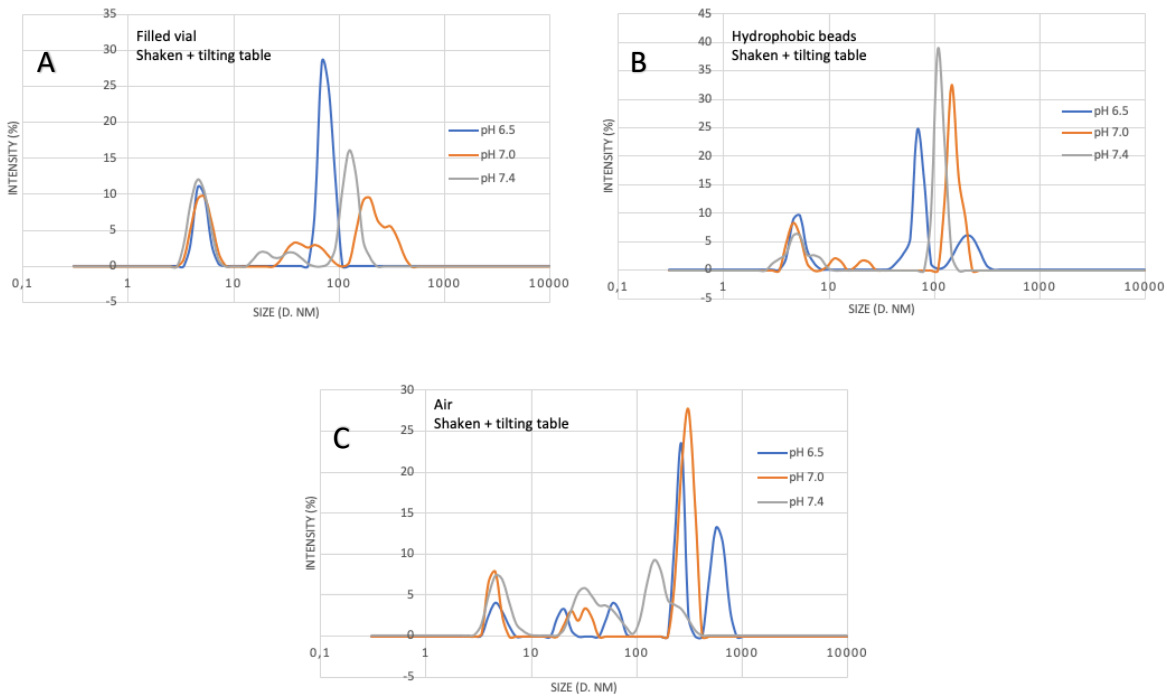

Figure 26 API with different surface interfaces and pH, all samples are shaken and placed on tilting table for 1 h. A. *Completely filled vial (i.e. no air).* ***B.*** *Hydrophobic beads.* ***C.*** *Air-water interface*

The size distributions of untreated API, Figure 23A - C, display a peak at ~100 nm which can also be seen in PSDs of treated API for all pH (Figure 24-26). As previously mentioned, it cannot be confirmed that the peak represents aggregates due to the lack of reproducibility

between measurements. However, if the peak is representative of larger aggregates it is not due to surface interfaces or pH.

There could be extremely small amounts of larger structures in the API samples, but it is not possible to prove if the structures are of proteinaceous nature or if they are results of other contamination, e.g. from buffer species or dust. As comparison, the volume PSDs of β-lg where heated sample was diluted with unheated sample (section 3.1.4) can be used (Figure 27). A sample with 20% heated β-lg shows a visible peak at ~24 nm in the volume distribution. The volume distribution with 5% heated and 95% unheated β-lg displayed a barely visible signal of the aggregates. Aggregates assuming the same size would thus need to exceed 5% to be detectable in the volume distribution.

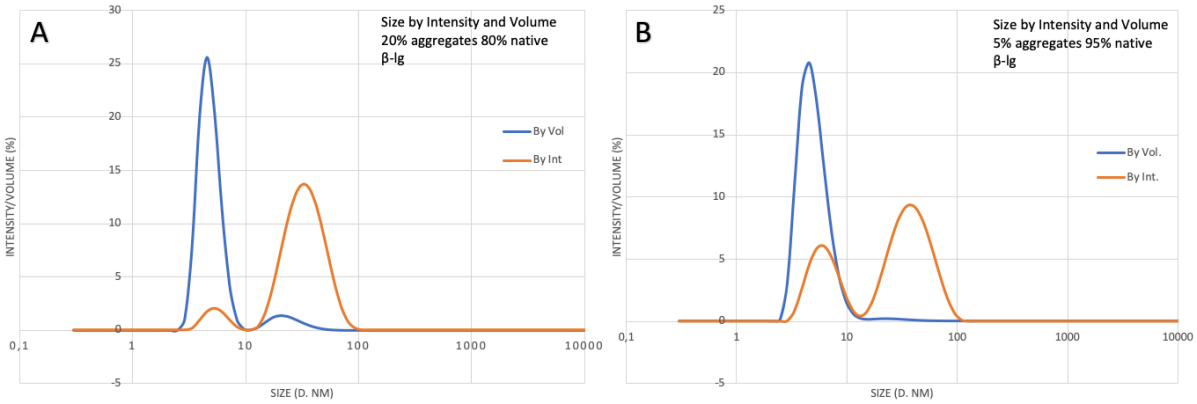

Figure 27 Size by Intensity and Volume PSDs of heated and unheated β-lg mixed to different ratios. A. *The aggregated ß-lg generates a detectable signal in both distributions.* ***B.*** *5% heated β-lg is barely visible in the Volume distribution*

If the reproducibility of the measurements of the API could be improved, one would not need to rely on the Size by Volume distributions to the same extent. Lack of reproducibility does not only occur between samples, but within the measurements of the same sample. Measurements of the API are displayed as single measurements and not average curves in Figure 28. Sizes beyond the peak representing the native protein structure (5 nm) appears to be drifting for each measurement. This supports the theory that these peaks are due to noise or contamination.

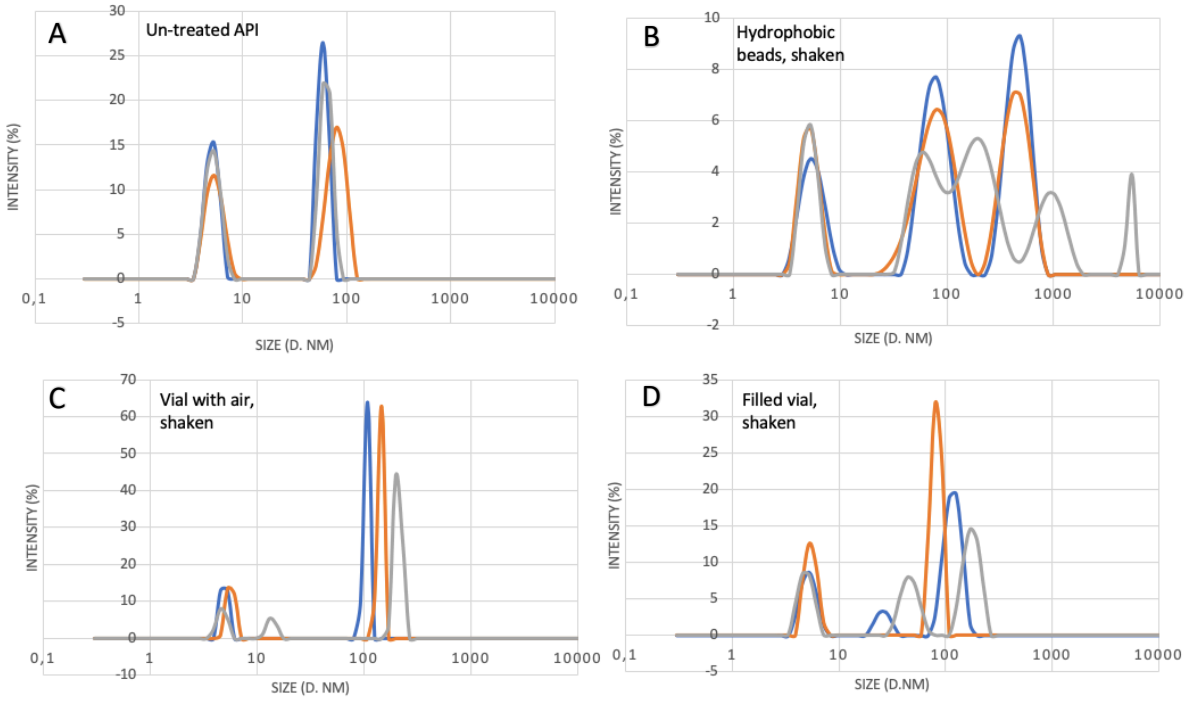

Figure 28 Measurements of the API are not reproducible. A-D. *Each measurement is shifted in the higher size range. Even though the peaks above 10 nm have been labeled as noise or contamination, the reliability of the PSDs is reduced.*

None of the formulations seem to have caused substantial aggregation based on the Size by Volume distributions. The correlograms, however, could indicate that there are larger particles in the sample due to a plateau in the decrease of the correlation function, but it cannot be concluded if it is due to aggregates or contaminants. Note that measurements of only buffer will still produce a PSD (Appendix 4). Two randomly selected correlograms are displayed in Figure 29. The PDIs of the measurements are higher than what is normally seen in monodisperse samples, i.e. below 0.2 (Table 9).

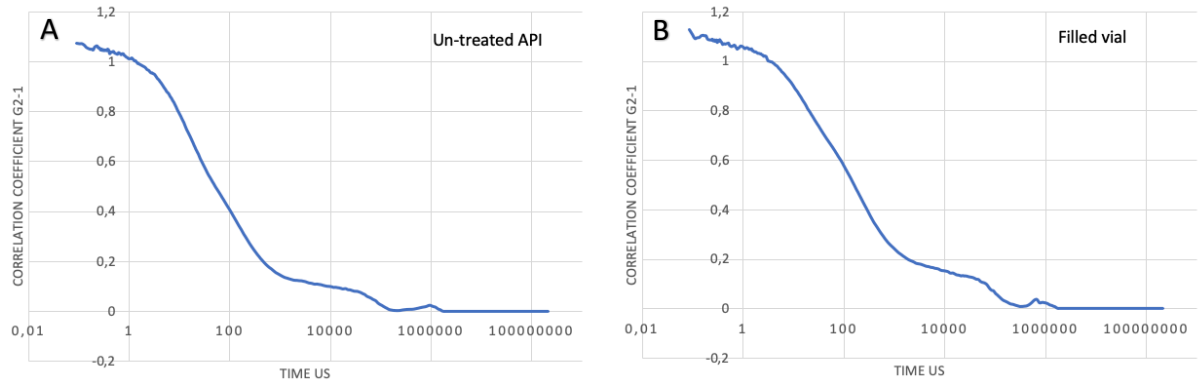

Figure 29 Two randomly selected correlograms from measurements with the API at pH 6.5. *Correlogram of untreated API* ***(A)*** *and filled vial* ***(B)*** *does not have an exponential decrease, which can indicate heterogenicity.*

Table 9 All treatments at the three different pH with corresponding PDI are listed. *PDI for all treatments are high and could be an indication of polydispersity.*

Physical treatment	Surfaces		pH	PDI
Shaken	Filled vial		6.5	0.472
	Air		6.5	1.29
		Hydrophobic beads	6.5	0.448
Tilting table	Filled vial		6.5	0.68
	Air		6.5	0.896
		Hydrophobic beads	6.5	0.711
Shaken	Filled vial		7.0	0.677
	Air		7.0	1.45
		Hydrophobic beads	7.0	0.582
Tilting table	Filled vial		7.0	0.43
	Air		7.0	1.06
		Hydrophobic beads	7.0	0.74
Shaken	Filled vial		7.4	0.493
	Air		7.4	0.502
		Hydrophobic beads	7.4	0.61
Tilting table	Filled vial		7.4	0.442
	Air		7.4	0.428
		Hydrophobic beads	7.4	0.792

4. Discussion

This master thesis aimed to assess the possibility of using dynamic light scattering to detect protein aggregation. When using the model protein β-lg to study aggregation the results seemed promising. Distinctions between aggregated and native protein could be made with both DLS and MADLS. When using the API, however, the same distinctions could not be made. Whether this was due to the characteristics of the protein such as instability (e.g. flexible folding affected by microenvironments) or lack of aggregates cannot be decided based on the results produced in this project. The most probable reason for poor reproducibility is, however, due to lack of successful aggregation.

Native β-lg assumes a dimeric configuration at pH 7 with an average diameter of 5 nm. The smallest size that can be detected by the Zetasizer Nano and Ultra instruments is stated as < 1 nm (Malvern 2020). It might be possible to detect particles of 1 nm, but the data is likely to be very noisy. When reaching smaller sizes, the signals produced by the particles are very weak. In intensity weighted distributions the contribution of a particle is proportional to $(size)^6$. If large particles are present in the sample, they will be detectable and generate a strong signal. A sample dominated by very small particles is therefore susceptible to detection of other particles, i.e. molecules from buffer might be given "relevance" by the weighting functions or pollutants as dust can dominate the spectra. A DLS measurement was done with only buffer to get an understanding of the underlying noise, see Appendix 4. Even though the PSD from the buffer cannot be superimposed with perfect fit to the noise in Figure 8B it becomes evident that the buffer does generate a signal that might interfere with the signal from the proteins. In these instances, it could be better to rely on volume or number distributions, unless the noise in the intensity distribution is of relevance. One could also increase the concentration when studying smaller particles. The quality of the results produced by DLS and MADLS increase at higher concentrations as judged by the correlograms with higher concentration of unheated β-lg.

DLS was measured with both Zetasizer Nano and Zetasizer Ultra. The instruments agree in the size values produced (z-avg and peak mean), but the width of the PSDs from Ultra are smaller than those generated by Nano. A narrower distribution or peak indicates a smaller span of sizes and could therefore be argued to be a more precise result. If aggregates and native protein are close in size, narrower distributions could be favourable for detection of aggregation due to better separation. As expected, the peaks by MADLS displays an even smaller peak width than DLS by the Zetasizer Ultra. MADLS utilizes three measurement angles which increases the resolution as well as the precision, which is reflected in peak width.

The size and shapes of aggregates can vary depending on what conditions they are induced (Nicolai *et al*. 2011). It was found that MADLS could differentiate samples with regards to peak mean for β-lg heated for 1 and 2 h whereas DLS could not. Various temperatures were also assessed (70, 75 and 80˚C) where both MADLS and DLS detected increased sizes of the aggregates with higher temperatures. Temperature seems to have a larger effect on particle size compared to incubation time, a comparison of sizes can be found in Table 10.

Table 10 Comparison between treatments of β-lg

Treatment	*MADLS (nm)*
2 h	34.3
70˚C (1 h)	30.1
75˚C	37.7
80˚C	41.2

Measurements of mixed samples (heated and unheated β-lg) showed that DLS with Zetasizer Ultra could detect a lower ratio of heat-treated sample than Zetasizer Nano (Figure 17C & D). The Zetasizer Ultra is a newer instrument where improvements of algorithms etc. have been made. These improvements include adaptive correlation which reduces noise by adapting shorter time runs and partitions correlograms based on appearance and statistical resemblance. Due to the improvements of the Ultra instrument, it is more resilient toward noise. MADLS did not provide any extra information in the measurements with mixed samples (heated ß-lg diluted with native). DLS can separate size populations with a ratio with respect to size of 3:1 whereas the improved resolution of MADLS can differentiate components with a 2:1 ratio (Malvern Panalytical 2018). Aggregated β-lg after standard treatment has a size range of about 20 – 60 nm and is in other words more than 3 times larger than dimeric, native protein (5 nm). DLS is therefore enough for separation of the two separate states. In the transition process, however, DLS cannot differentiate between sub-populations (Figure 18). After 15 min of heating the near-in-size particles are closer than a 3:1 ratio and the proteins are therefore grouped together in the PSD by DLS. The higher resolution of MADLS allows separation of the two.

There is a threshold for detection of aggregation with the volume distribution. In Figure 28 the volume PSD does not show a clear peak for the aggregates at 5% of heated sample and 95% unheated. If the intensity weighted spectra is not reliable in itself when studying aggregation and the volume distribution is needed, one should aim to obtain a higher ratio of aggregates than 5%. Once interpretation of intensity distributions has been clarified, one can rely on it for detection of aggregation. The need of two spectra with different weights (intensity and volume) is a drawback of the technique, it is not always possible to produce aggregates of the same size exceeding the 5% threshold as seen with the API.

Moreover, the lowest limit of detection in combination with measurement volume was investigated. With the Zetasizer Ultra instrument one can use a capillary cuvette (3 µL) for sizing measurements. Measurements with heated β-lg could produce reliable results with a concentration of 0.5 mg/mL in the capillary cuvette, lower concentrations resulted in noisy correlograms (Figure 19). A bigger volume (1 mL) produce reliable results at 50 µg/mL. There is a trade-off where one can either choose to use a lower concentration and higher volume, or higher concentration and a smaller volume. The same reasoning goes for the unheated β-lg where 0.5 mg/mL can be used in 1 mL measurements and 1 mg/mL with the capillary cuvette.

DLS and MADLS are indirect measurements of particle size (e.g. measurements are based on signals proportional to the size), so complementary techniques should be used in parallel in the process of getting familiar with a protein. Confirming the results by orthogonal techniques should be a standard approach in initial DLS measurements with a new protein. The TEM images from Vironova (Figure 12) does confirm the results from DLS and MADLS and supports the accuracy of the results. As mentioned in Methods, some TEM images are not presented in the report due to time restraints in imaging. Once images are taken it is our hope that the images can be used continuously as a compliment and validation of DLS measurements.

The experimental trials with an API aimed to set up a formulation by assessing different pH and various surface interfaces (hydrophobic beads, air and air-bubbles, vial) as well as physical treatments (shaking and tilting table) to investigate parameters that induce aggregation. Despite efforts in creating an environment where aggregation could be monitored, consistent aggregation could not be established.

The incoherent PSDs generated for the API was difficult to interpret. Un-aggregated β-lg did also produce some noisy data but not to the same extent. β-lg and the API are in the same size range, but the API is a lot more unstable. Both proteins have a globular shape which should be advantageous when using DLS since the technique assumes spherical shapes. The instability of the API might lead to a partial and non-uniform loss in native shape and thus generate more noisy PSDs. Moreover, peaks appear at ~100 nm in all intensity PSDs of the API without specificity to treatment and formulation. Why this peak is displayed in all intensity distributions cannot be explained as aggregation due to the lack of repeatability between measurements. The peak could be appearing due to simply chance from noise or signal from molecules in buffer (Appendix 4). It cannot be completely ruled out, however, that the fluctuating peaks are aggregates. The model protein β-lg produced uniform aggregates, which is commonly not the case. If aggregates are present in the API it is not due to the different surfaces since the same pattern of fluctuating peaks can be seen in measurements done on untreated samples. What should be pointed out is that the peak at ~100 nm and the quality of the measurements is not improved by MADLS, Appendix 6.

The supplier informed that the products on the market of the API has pH 6 and 6.5 where aggregation is not expected. Lowering the pH further and/or increasing the ionic strength should according to suppliers result in aggregation.

The stability of the API was assessed at pH 6.5, 7.0 and 7.4. The samples were measured twice with 1 h apart. Aggregation could not be verified, but between measurements the intensity at the size of native protein was reduced. It was realized that every pH was higher than intended due to pre-treatments of the API in the freeze-drying process where it becomes slightly basic which will increase the pH of the formulation. The real pH values were measured to 6.9, 7.2 and 7.6. At a pH close to 7 the API should be sufficiently charged to avoid aggregation. The formulation with pH 6.5 was hypothesized to have a higher degree of aggregation than 7.0 and 7.4. To obtain a formulation with the desired pH, one would need to test several pH and measure

the end pH after dissolving the API. Adjusting the pH after dissolving the protein would lead to precipitation according to the supplier of the API.

Interfaces and surfaces chosen to destabilize the API was air, hydrophobic beads and the glass vial. Hydrophobic surfaces are generally seen as risk factors for aggregation when working with proteins. Proteins fold into characteristic functional structures where the hydrophobic residues are commonly buried within the core of the structure. Interactions with the surface destabilizes the protein structure by creating an environment where new interactions between surface and protein can alter the configuration of the protein structure. It was therefore of interest to investigate how the surfaces and interfaces affected the API. The air-water interface has also been assessed as a risk for aggregation. The shear force of shaking the APIs is a risk factor that can generate aggregates which is why the samples were shaken by hand before being placed on tilting table. The results indicate that the protein adsorbed onto the surface, but no evidence of progressed aggregation in the solution could be seen with DLS. The PSDs generated after previously mentioned treatments did not look different from untreated PSDs, meaning that surface induced aggregation could not be observed.

Protein samples with air and hydrophobic beads does display a lower signal of native protein after being placed on a tilting table. The tilting table allows circulation of the sample and the contact between surfaces/protein and adsorbed protein/protein is therefore increased. In Appendix 7, intensity distributions of samples at pH 6.5 are displayed after shaking and after 1 h on tilting table. The intensity of the ~5 nm peak is lower after tilting table which agrees with the continuously renewed protein-interface interactions ultimately leading to more protein adsorption.

Lastly, the PDI of all API measurements are very high which generally indicates that a sample is polydisperse (Table 9). This, together with the correlograms implies that there is more than one population in the API samples, over all treatments and every pH. The PDI of filtered API was 0.394 in comparison to unfiltered from same sample batch 0.349. To obtain a clean, monodisperse sample before treatment one would need to test more filtration methods.

5. Conclusion

The results show that DLS and MADLS are efficient techniques for detection of aggregation when there is a high enough proportion of aggregates (5%). Decrease in signal for native protein between measurements can be used as an indicator for changes in the state of a protein such as adsorption and/or aggregation but more experiments need to be done prove the correlation. MADLS produces more reliable particle size estimates than DLS due to its higher precision, but DLS is sufficient in detection of aggregation if the size difference between native and aggregated protein is big enough.

6. Acknowledgments

I would like to thank my two supervisors Linnea Enstedt and Ulla Elofsson for supporting me through the project. You were always there for me with guidance, help and discussions. I truly could not have asked for better supervisors.

Thanks to Kushal Sejwal for supplying me with TEM images from Vironova and for teaching me about the technique.

Big thanks to all my colleagues at RISE for your immediate willingness to help and for the positive experience you have all given me.

Thanks to Amanda Västberg for assisting me in the lab, it was a pleasure to work with you.

I would also like to thank my subject reviewer Maria Selmer for your valuable comments and insightful knowledge.

Thanks to Ferring for scientific input.

Lastly, I would like to thank NextBioForm for letting me be a part of their innovations.

References

Arenas-Guerrero, P., Delgado, Á.V., Donovan, K.J., Scott, K., Bellini, T., Mantegazza, F., Jiménez, M.L., 2018. Determination of the size distribution of non-spherical nanoparticles by electric birefringence-based methods. Scientific Reports 8, 9502. https://doi.org/10.1038/s41598-018-27840-0

Bauer, R., Hansen, S., n.d. Detection of Intermediate Oligomers, Important for the Formation of Heat Aggregates of -Lactoglobulin 8.

Berrill A, Biddlecombe J, Bracewell D. 2011. Product Quality During Manufacture and Supply. Peptide and Protein Delivery, pp. 313–339. Elsevier,

Blake S, Amin S, Qi W, Majumdar M, Lewis EN. 2015. Colloidal Stability & Conformational Changes in β-Lactoglobulin: Unfolding to Self-Assembly. International Journal of Molecular Sciences 16: 17719–17733.

Croguennec T, O'Kennedy BT, Mehra R. 2004. Heat-induced denaturation/aggregation of β-lactoglobulin A and B: kinetics of the first intermediates formed. International Dairy Journal 14: 399–409

Cox, S. 2007. Proteins: Hormones, Enzymes and Monoclonal Antibodies - Background. *Handbook of pharmaceutical biotechnology.* New Jersey: Wiley-Interscience, 691-737.

Elofsson, U. 1996. Protein Adsorption in Relation to Bulk Phase Properties-ß-Lactoglobulins in solution and at the Solid/Liquid Interface. Diss. Lund University.

Fink, A.L., 1998. Protein aggregation: folding aggregates, inclusion bodies and amyloid. Folding and Design 3, R9–R23. https://doi.org/10.1016/S1359-0278(98)00002-9

Kelly P, Woonton BW, Smithers GW. 2009. 8 - Improving the sensory quality, shelf-life and functionality of milk. In: Paquin P (ed.). Functional and Specialty Beverage Technology, pp. 170–231. Woodhead Publishing,

Leurs U, Mistarz UH, Rand KD. 2015. Getting to the core of APIs – Comprehensive structure analysis by mass spectrometry. European Journal of Pharmaceutics and Biopharmaceutics 93: 95–109.

Malvern Panalytic, 2020. Improved component resolution with Multi-Angle DLS (MADLS). https://www.malvernpanalytical.com/en/learn/knowledge-center/whitepapers/WP180926ImprovedComponentResolutionMADLS (Visited 15-03-2020)

Malvern Panalytical, 2018. Adaptive Correlation: Better DLS with less time and effort. Application note.

McGovern, M. E., Kullury, K. M. R., Thompson, M., 1994. Role of solvent on the Silanization of Glass with Octadecyltrichlorosilane. Langmuir 10, 3607-3614.

Nicolai T, Britten M, Schmitt C. 2011. β-Lactoglobulin and WPI aggregates: Formation, structure and applications. Food Hydrocolloids 25: 1945–1962.

Ockenga, W. 2011. Phase contrast. If two waves interfere, the amplitude of the resulting Leika Science Lab. https://www.leica-microsystems.com/science-lab/phase-contrast/ (Visited 2020-03-12)

Pecora R. Dynamic Light Scattering Measurement of Nanometer Particles in Liquids. 9. The principles of dynamic light scattering :: Anton Paar Wiki. WWW document: https://wiki.anton-paar.com/en/the-principles-of-dynamic-light-scattering/. Accessed 5 February 2020.

Price, N. C, Nairn J. 2009.The important properties of proteins and how to explore them. *Exploring proteins*. Oxford: Oxford University Press.

Quianzon CC, Cheikh I. 2012. History of insulin. Journal of Community Hospital Internal Medicine Perspectives, doi 10.3402/jchimp.v2i2.18701.

Roberts CJ. 2014. Protein Aggregation and Its Impact on Product Quality. Current opinion in biotechnology 0: 211–217.

Sava N, Van der Plancken I, Claeys W, Hendrickx M. 2005. The Kinetics of Heat-Induced Structural Changes of β-Lactoglobulin. Journal of Dairy Science 88: 1646–1653.

Solá RJ, Griebenow K. 2009. Effects of glycosylation on the stability of protein pharmaceuticals. Journal of Pharmaceutical Sciences 98: 1223–1245.

Stetefeld, J., McKenna, S.A., Patel, T.R., 2016. Dynamic light scattering: a practical guide and applications in biomedical sciences. Biophys Rev 8, 409–427. https://doi.org/10.1007/s12551-016-0218-6

Wang W, Nema S, Teagarden D. 2010. Protein aggregation—Pathways and influencing factors. International Journal of Pharmaceutics 390: 89–99.

Wang, W., Roberts, C.J., 2018. Protein aggregation – Mechanisms, detection, and control. International Journal of Pharmaceutics 550, 251–268. https://doi.org/10.1016/j.ijpharm.2018.08.043

Weetall, H. H., 1996. Preparations of immobilized proteins covalently covalently coupled through silane coupling agents to inorganic supports. Advances in Molecular and Cell biology 15A, 161-192. ISBN: 0-7623-0114-7

Appendix 1. Preparation of ß-lg samples

Phosphate buffer with 0.02% NaAz, pH 7

Make two 50 mM solutions, one for the monobasic (H_2NaPO_4) and one for the dibasic (HNa_2PO_4) and then mix them until pH 7 is reached.

The salts were dissolved in 100 mL Milli-Q water by stirring for about 15 min. When salts were dissolved, Milli-Q water was added to a final volume of 200 mL. The 50 mM solutions were then mixed (about 40% of monobasic, 60% dibasic) to reach pH 7. Final volume was measured to 270 mL and the buffer was then filtered through 0.22 µm filters into a flask.

Sodium azide (NaAz) was added to the buffer. Stock concentration was 2%, final concentration was to be 0.02%.

Calculations

$$Mw(H_2NaPO_4 \bullet H_2O) = 156.01\ g/mol$$
$$V = 200\ mL = 0.2\ L$$
$$m = Mw \times V \times c = 156.01 \times 0.2 \times 0.05 = 1.56\ g$$

$$Mw(HNa_2PO_4 \bullet H_2O) = 177.99\ g/mol$$
$$V = 200\ mL = 0.2\ L$$
$$m = Mw \times V \times c = 177.99 \times 0.2 \times 0.05 = 1.78\ g$$

Procedure with ß-lg

A beaker was filled with water and brought to a 70ºC water bath. 60 mg of ß-lg was dissolved in 6 mL buffer (10 mg/mL), note vial was pre-rinsed with Milli-Q. The protein was allowed to dissolve in room temperature for 10 minutes and was then filtered through 0.22 µm filters to remove any particles that had not dissolved. 2.5 mL was saved as unheated and placed in the fridge, and 2 mL was heated at 70ºC for one hour. Heated sample was then placed on ice for 10 min and were then equilibrate to room temperature.

Dilution series was made for heated and unheated samples where 300 µL of protein solution was added to 2.7 mL of buffer (1:10 dilution).

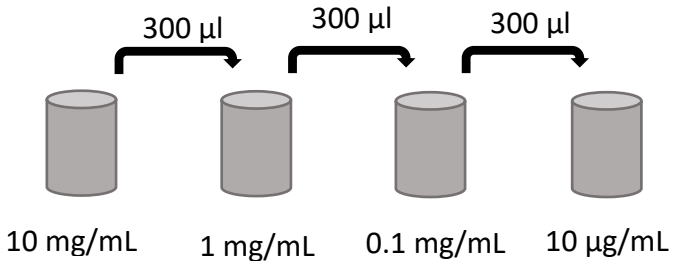

Appendix 2. Preparation of API

10 mM phosphate buffer with 0.02% NaAz

50 mM phosphate buffer (Appendix 1) was diluted to 10 mM with Milli-Q. Three different pH were prepared: 6.5, 7.0 and 7.4. NaAz was added to each buffer to a final concentration of 0.02% (stock concentration 2%). The buffers were filtered through 0.22 µm before usage.

The API was stored in smaller freeze died aliquots in -20˚C. Vials with the API was taken out from freezer 20 min before being dissolved to a final concentration of 3 mg/mL. They were kept under an aluminium foil covered beaker since the protein is light sensitive. Protein is very porous and light, so when adding buffer, it was done very slowly and along the sides of the vial. Mixing of the sample was done according to standardization of the suppliers: with the bottom of the vial against solid surface it was spun 10 laps and was then carefully tilted and slowly twirled once.

Treatments

4 mL vials were rinsed with Milli-Q and left up-side-down on dust free paper until dry. Three treatments were made: air-water interface (1), contact with hydrophobic beads (2) and one vial filled all the way to the top with protein sample (i.e. no air) (3). Lids of the vials are made from plastic and the inside of the lid is coated with aluminium. A 4 mL vial has a volume of about 5 mL.

1. 2 mL of protein was added to vial which leaves about 3 mL air. The sample was shaken by hand for 10 s and air bubbles were produced.
2. Empty vial was weighed before adding beads and then weighed again after addition. About 5 g of beads would allow 1.5 mL of protein sample to fit in the vial. Protein sample was added all the way up to the top.
3. Vial was filled all the way to the top with protein sample.

Surface area of beads

The average weight of one bead was calculated by weighing 52 beads to 0.0457 g

$$\frac{0.0457\ g}{52} = 8.78 \times 10^{-4} g/bead$$

Surface area was then calculated with the equation below where r is the radius (1 mm) and W_B is the total weight of beads.

$$4\pi \times r^2 \times \frac{W_B}{0.088}$$

$$4\ \pi \times r^2 \times \frac{5000\ mg}{0.878\ mg} = 71\ 562\ mm^2 = 716\ cm^2$$

Appendix 3. Definition of a correlogram of good quality

A correlogram of good quality should have a clear correlation at the beginning of a measurement, e.g. a small τ, followed by exponential decrease as τ increases. The correlogram reaches the baseline when there is no longer any correlation.

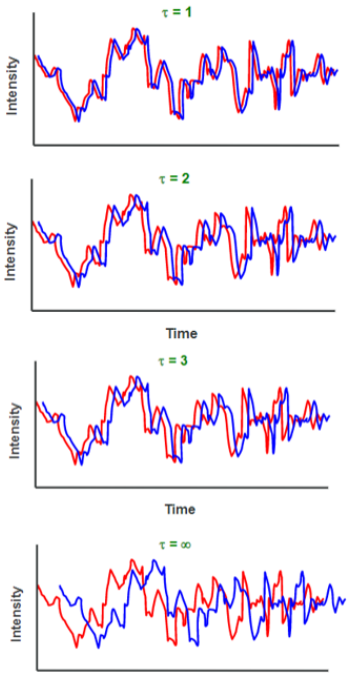

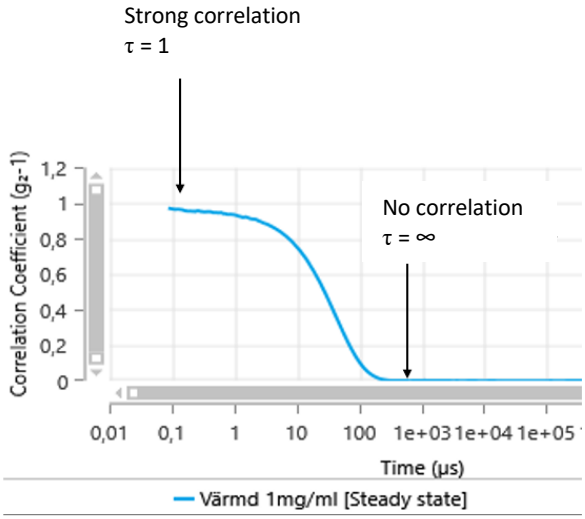

Appendix 4. Intensity-weighted size distribution of buffers

PSDs generated from measurements with only buffer. Even though there are no particles dissolved in the buffer, visible signals are produced.

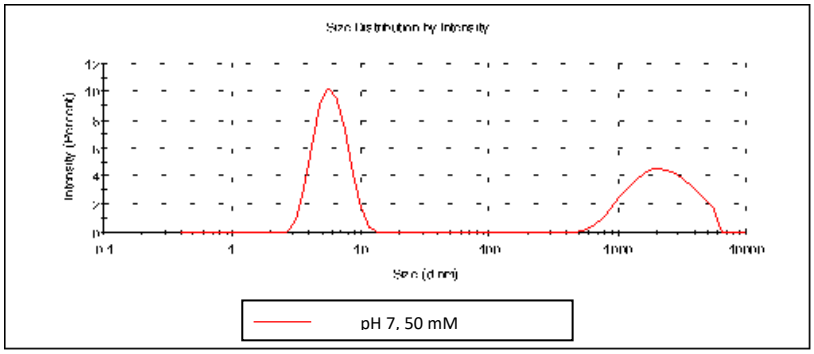

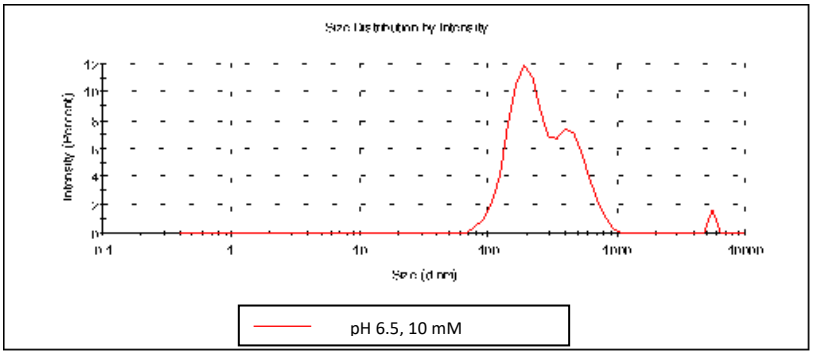

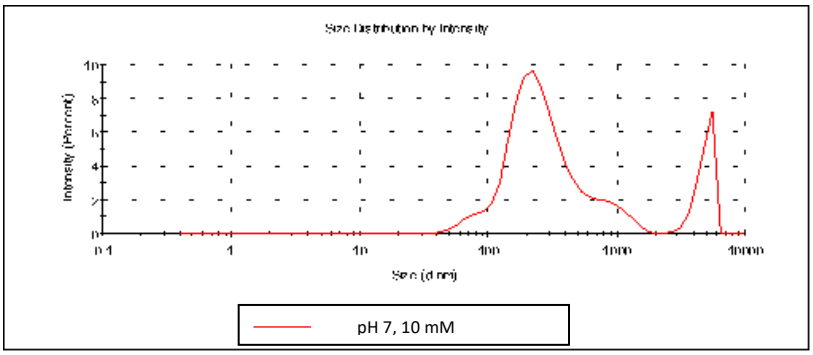

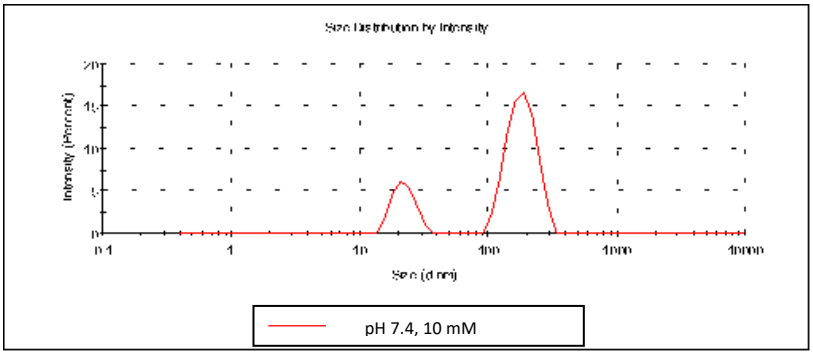

Appendix 5. All treatments of API plotted according to pH

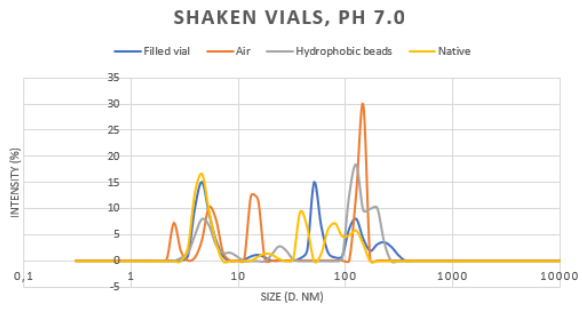

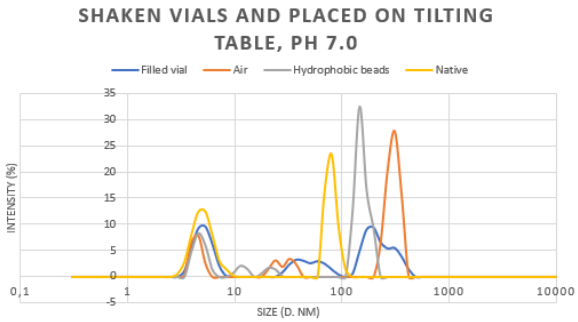

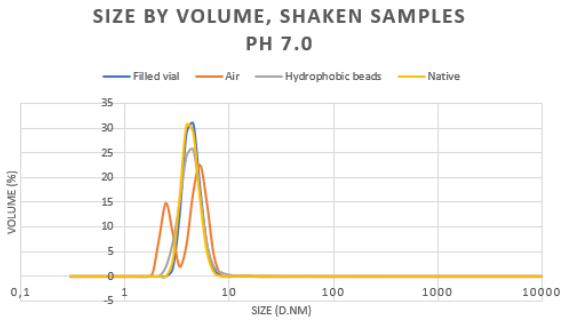

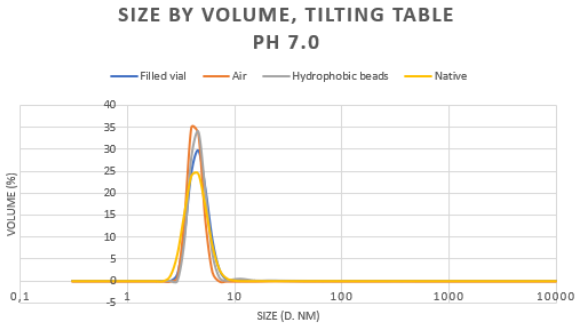

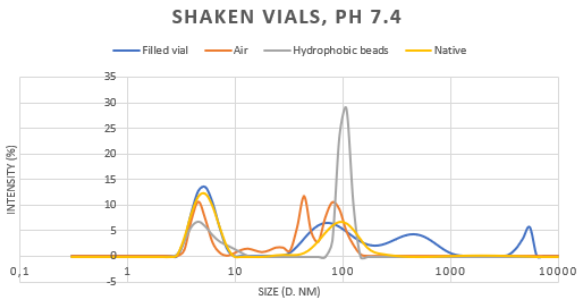

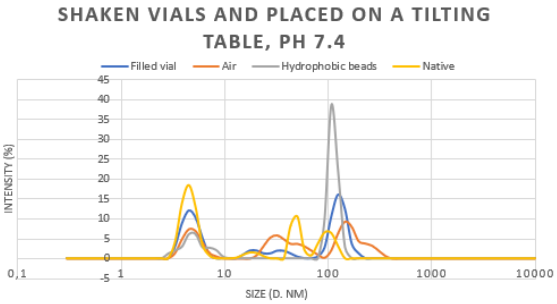

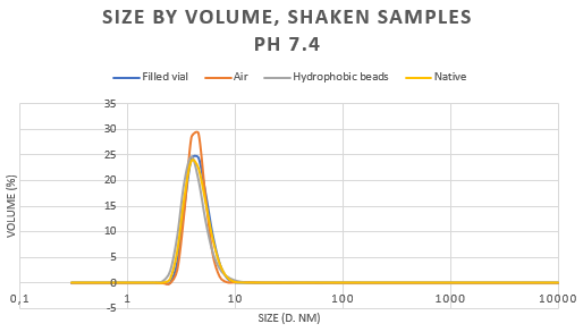

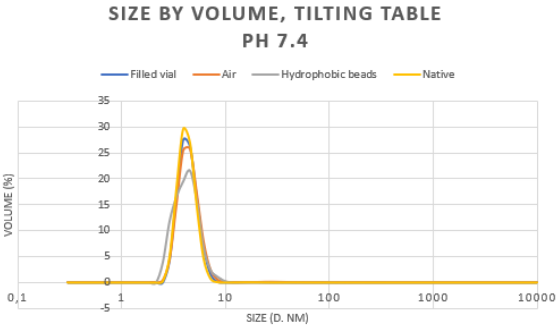

Appendix 6. MADLS measurement of API in pH 7.4

Using MADLS did not improve the quality of the measurement of the API.

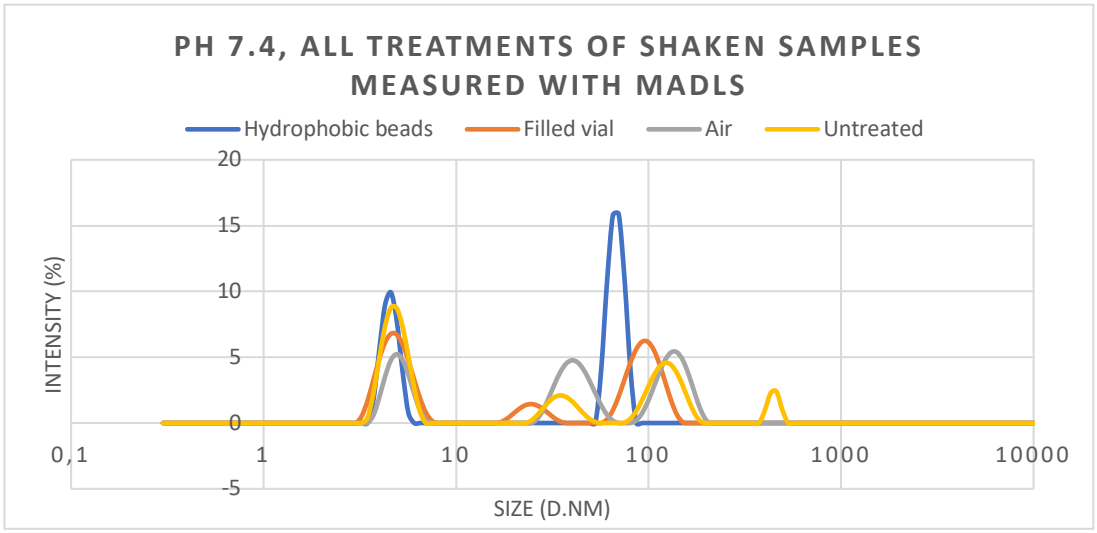

Appendix 7. Intensity-weighted size distributions of API after treatments

Intensity at native size decreased after sample was placed on tilting table. Possible explanation is increased adsorption